Geochemical and isotopic investigation into the tectonic setting of Mesoarchean and Paleoproterozoic granitoid suites within the eastern Gawler Craton, South Australia

Stacey Goodwin

(1161140)

Supervisor: Karin Barovich

25/10/10

ABSTRACT

A geochemical study into a recently identified Mesoarchean Archean granitoid suite in the Eastern Gawler Craton, South Australia, has found that over a larger area the geochemistry and isotopes are variable. Granitoids of ~3240Ma have been dated using the SHRIMP, which look identical to the cooyerdoo but have trondhjemitic REE patterns. This study has used geochemical and Nd-Sm isotopic data to identify the tectonic setting and source region of Mesoarchean (~3150Ma) granitoids and amphibolites and Paleoproterozoic (~1730Ma) granitoids and amphibolites. The old and young granites are high K, Calc-alkaline, I type granites and are interpreted to have formed in a continental arc setting. There are a few enriched younger and older enriched mafics formed by metasomatism of the mantle. The ~3240Ma and ~3150Ma are interpreted to have been formed by the same tectonic event. This study has shown the eastern Gawler Craton to be even more complex than was thought from the Fraser *et al.* 2010 study.

Table of Contents

INTRODUCTION

Granitoids formed in different tectonic settings tend to have different rock types, geochemistry and associated minerals within the different granite (for example hornblende bearing or muscovite bearing). Orogenic granitoids (formed during mountain building events and associated with subduction) can occur in oceanic island arcs, continental arcs and continental collision. Anorogenic granitoids form at continental rifts, hot spots and mid-ocean ridges and are caused by magmatism that occurs at tectonic plate spreading margins or within plate and form in the absence of orogenic events. Transitional granites are caused by post-orogenic uplift or collapse (Maniar & Piccoli 1989; Winter 2001). Continental and oceanic crust is formed and recycled and new crust made via tectonic processes associated with the Wilson Cycle. Specific types of granites form at different stages of the cycle due to different tectonic processes and different sources being available. More than one granitoid type can occur in a given geological setting and most settings are distinguished by an association of granitoids (Barbarin 1999). Changes in granites through time can tell us about the evolution of the lithospheric column from which the granites are being sourced.

The tectonic settings rocks were formed in can be constrained using geochemistry and isotope chemistry (Bonin 1990; Eklund *et al.* 1998; Peterson *et al.* 2002; Clemens *et al.* 2006). The geochemistry and tectonic settings of Phanerozoic rocks are often used to infer the tectonic setting of Precambrian rocks as is the association of the Precambrian rocks with tectonic events occurring at the time of formation (Foden *et al.* 1988; De *et al.* 2000; Whalen *et al.* 2004).

Granitoids can be formed by the differentiation of continental crust melts, from mantle melts or from the mixing of continental and mantle melts (Petford *et al.* 1997; Frost *et al.* 2001). The generation of granites is controlled by the mantle and is a four step process: 1) melting, 2) segregation of the melt 3) ascent and 4) emplacement (Petford *et al.* 1997). The formation of granites occurs at plate boundaries in the Pahnerozoic, preferentially (Vigneresse 2004).

Mafic magmas can become enriched by crustal assimilation, where rocks from the walls of the magma chambers are assimilated into the magma; the mixing crust and mantle; or metasomatism where the mantle becomes 'selectively' enriched due to the water-melts of a subducting slab (Yang *et al.* 2004). This enrichment in the magmas can cause the resulting rock to have enriched geochemical signatures, which are more like continental crust geochemical signatures.

In the Archean the most common granitoid type was the juvenile tonalite-trondhjemite-granodiorite (TTG) (Glikson 1979; Condie 1993). Other granitoid suites also existed during the Archean. The TTG dominance decreased by the end of the Archean when re-working of continental crust became more predominant (Martin 1994).

A Mesoarchean granitoid crust beneath the Gawler Craton has been inferred by many researchers (Creaser & Fanning 1993; Daly & Fanning 1993). This inference was based on inherited zircons being found within younger magmatic and sedimentary rocks, respectively. Creaser & Fanning (1993) identified inherited zircons within the

Charleston Granite (1585 ± 5 Ma), in the eastern Eyre Peninsula. One of these zircons had a ^{207}Pb-^{206}Pb age of 3149 ± 15 Ma. This led Creaser and Fanning to suggest that crustal material ≥ 2600Ma and possibly as old as ~3150 Ma had been a part of the source from which the Charleston granite formed (Creaser & Fanning 1993). Detrital zircons with an age of ~3100Ma were found within the Paleoproterozoic sediments of the Labrynth Formation within the Gawler Craton (Howard, unpub data).

Prior to Fraser *et al.* (2010), the oldest known rocks in the Gawler Craton were the 2560Ma Devil's Playground Volcanics (Swain *et al.* 2005b). The discovery of an actual rock, the Cooyerdoo Granite, with an age of ~3150 Ma increased the age of the Gawler Craton by 500 billion years. This granite was dated as part of Primary Industries and Resources South Australia's (PISRA) geological mapping program and geochronology associated with the Geoscience Australia deep crustal seismic experiments (Korsch & Kositcin 2010).

The South Australian Heat Flow Anomaly (SAHFA) is an area of elevated heat flow within the eastern Gawler Craton, with heat flow increasing from west to east (Neumann *et al.* 2000). The SAHFA is caused by the crust being enrichment in heat producing elements. The heat flow of the Cooyerdoo Granite was calculated to have a mean value of ~5.00 μWm^{-3} (Fraser *et al.* 2010). The Cooyerdoo Granite is relatively enriched in radiogenic elements and the Cooyerdoo Granite possibly being under the SAHFS is a possible cause of the heat production anomaly (Fraser *et al.* 2010). The Burkitt Granite and the Charleston Granite with surface heat productions of 17.0μWm^{-1}

and 11.1 μWm^{-1}, respectively, have the two highest heat production values in the Gawler Craton (Neumann 2001). The Burkitt Granite and the Charleston Granite intrude the Mesoarchean crust and have been inferred to have been at least derived formed from it (Fraser *et al.* 2010). In order to understand the possible tectonic setting of the Mesoarchean and younger granite rocks in the eastern Gawler Craton, and to understand how they may be related to the SAHFA, whole rock geochemical and Sm-Nd isotopic data have been collected during this study.

As well as looking at the Mesoarchean granites, this study will also look at the Mesoarchean mafic rocks and younger (1735Ma) group of granite and mafic rocks from the same area. These granitoids and amphibolites are formed from the same lithosphere but with a 500 million year interval between the two associations. The continental crust during the Archean was very young and hot and these rocks will be able to tell us about continental growth in the Mesoarchean and Paleoproterozoic. They will also be able to tell us about the lithospheric evolution of the sample area and the possible tectonic setting. This study will extend the knowledge of the history of the Gawler Craton.

GEOLOGICAL SETTING

South Australia consists of two Precambrian cratons: the Gawler Craton and the Curnamona Craton, which are separated by the Adelaide fold belt (Figure 1) (Paul *et al.* 1999). The Gawler Craton had previously been thought of as a late Archean to early Proterozoic core encompassed by Paleo- and Mesoproterozoic rocks (Hand *et al.* 2007). At its north boundary the Gawler Craton is covered by the sedimentary Neoproterozoic

Officer Basin and to the west by the sedimentary Cenozoic Eucla Basin. The Stuart Shelf is Neoproterozoic in age and consists of sediments and covers the north eastern regions of the Gawler Craton (Parker 1993). Due to sedimentary cover the Gawler Craton is poorly understood (Swain *et al.* 2005a).

The Galwer Craton has undergone four major orogenic events: the Sleaford Orogeny (2460-2430Ma), Cornian Orogeny (~1860-1850Ma), the Kimban Orogeny (1730-1630Ma) and the Kararan Orogeny (1595-1575Ma) (Reid *et al.* 2009). The Kimban Orogeny is the main orogeny of interest in this study, and caused metamorphism of amphibolite to granulite facies, formed the syn-post orogenic Moody Suite (Schaefer 1998) and formed the Kalinjala Shear Zone (KSZ). The KSZ is a high strain shear zone of more than 200 km long (Parker 1980) and is a large structure in the eastern Eyre Peninsula (Vassallo & Wilson 2002). The KSZ formed around 1730-1700 Ma during dextral transpression of the Kimban Orogeny (Swain *et al.* 2005a). The Hiltaba Suite formed from 1595-1575Ma (Hand *et al.* 2007). The Hiltaba Suite has high heat production (Neumann *et al.* 2000). The metamorphic, sedimentation and orogeny history of the eastern Gawler Graton is shown in Figure 2.

The Mesoarchean granitoids are located in the eastern Gawler Craton, South Australia, where they form basement to the iron-rich sediments of the Middleback Ranges. The current known extent of the Mesoarchean granitoids is between Iron Knob and Iron Baron mines and has an area of ~20km x 30km (Figure 3). The extent of this outcrop is unknown but is thought to be much larger and be at least ~1500km^2. Fraser *et al.* (2010)

suggests that the KMZ is the western extent of the Mesoarchean crust. The Middleback Ranges is an important iron ore district for South Australia and for over a century iron ore has been mined there and is still being mined today. Banded Iron formations have been mined for iron ore in this region since the early 1900s (Yeates 1990). The Mesoarchean granitoid suite had previously been mapped as Paleoproterozoic Lincoln Complex (Parker 1993). Though there is currently no geochronological data it is possible that the Mesoarchean granitoid basement may extend across some of or the rest of the Gawler Craton (Reid *et al.* 2009).

The Cooyerdoo Granite could be basement to the Middleback Subgroup (iron-bearing sediments) or there could have been a fault that could have juxtaposed them. The Cooyerdoo Granite being basement to some parts of the Gawler Craton could explain the inherited zircon found by Creaser and Fanning (1993) in the Charleston Granite and may have been caused by the Charleston Granite intruding through or being in part remelted from the Cooyerdoo Granite or an equivalent rock. The Cooyerdoo Granite has been described as being relatively weakly deformed a rock so old and the zircon data by Fraser *et al.* (2010) show no isotopic disturbance or zircon growth caused by the Sleafordian, Cornian, Kimban or Hiltaba (Fraser *et al.* 2010). A possible reason for this is that the Cooyerdoo did not experience high metamorphic conditions possibly due to them being located at a shallow crustal level.

FIELD RELATIONSHIPS

Two associations were seen in the field: the older Cooyerdoo Granite plus unnamed gneissic granite and associated amphibolites (intermediate to mafic rocks) that were likewise gneissic in character; and the younger, weakly deformed pink granites and associated weakly deformed and intermingled amphibolites.

The Cooyerdoo Granites (Figure 4a) and unnamed gneissic granites appear to be end member of one unit, as no contact between the two was seen. There was an area where the two seemed to transition into each other. The pink unnamed gneissic granite seemed to transition into pink Cooyerdoo Granite, which seemed to transition into grey Cooyerdoo Granite. There is some segregation (compositional) within the unnamed gneissic granite (Figure 4b) probably caused by segregation in the melt or when the rock was deformed. The Cooyerdoo Granite and unnamed gneissic granite are found near amphibolite. The unnamed gneissic granite was observed in a mylonite zone with amphibolites (Figure 4c), where the unnamed gneissic granite appeared darker, possible due to it containing some more mafic minerals.

The older amphibolites were defined largely on the basis of their proximity to the Cooyerdoo or unnamed gneissic granite and because they invariably showed some degree of gneissic foliation, whereas the amphibolites from the inferred younger association did not show such degree of recrystallisation and, more importantly were sampled where we could see they were intermingled with the younger association

granites. The separation between younger and older mafic is qualitative in most instances except for the inferred younger mafic that was dated.

SAMPLES AND PETROGRAPHY

The locations of the samples in this study are shown in Figure 3. For each sample whole rock geochemistry is shown in Table 2.

Cooyerdoo and unnamed gneissic granite (Samples 1723505, 1723506, 1723507, 1723508, 1723509, 1723513, 1723529, 1721025, 1721026)

The Cooyerdoo Granite is a medium grained quartz, plagioclase, biotite and hornblende gneissic granite with a grey appearance (Figure 4a). The unnamed gneissic granite (Figure 4b) is a medium grained quartz, plagioclase, k-feldspar, biotite and hornblende gneissic granite with a pink appearance.

Young Pink Granite (Samples 1723516, 1723517, 1723530, 1721027, 1723527, 1723524)

The pink granite (Figure 4d & 5b) is medium grained containing mostly quartz, K-feldspar and plagioclase but also has some biotite. It has quartz grains of up to 0.5mm and the rest of the grains are smaller. The pink granite (1721027) was observed as isolated rock out crops and sometime as rubble. Importantly, in one locality, the

unnamed gneissic granite occurred as an encave within the pink granite, suggesting the latter may have been derived from, or partially assimilated the unnamed gneissic granite.

Old and Young Amphibolites (old samples: 1723511, 1723518, 1723519, 1723520 and young samples: 1721028, 1723523, 1723526, 1723515)

The older and younger amphibolites were classified based on their special relationship to the older and younger granitoids. The older amphibolites (Figure 5d) are foliated, coarse grained, hornblende and plagioclase rich amphibolites with clinopyroxene. There are two types of young amphibolites. The first (1723528 and 1723515) is an amphibolite (Figure 4e) consisting mainly of fine grained hornblende and fine to medium grained plagioclase. Sample 1723515 contains biotite and has finer grained plagioclase which defines a foliation. Sample 1723528 has "blobby" plagioclase and has no foliation. The second group are samples 1721028 and 1723526 (Figure 4f) are plagioclase and hornblende rich, foliated amphibolite with small amounts of quartz. Sample 1721028 has been multiply deformed and shows a fabric and microshears angled at 25-40^{o} to the fabric (Figure 5c).

Age (U-Pb SHRIMP)

PIRSA, using Geoscience Australia's SHRIMP in Canberra, have dated four samples as part of a regional geochronology program in collaboration with Centrex Metals Ltd. The results of these four samples have not been published as yet, however, the results have been provided as a personal communication by E. Jagodzinski (PIRSA) since they are

directly related to the samples analysed in the present geochemical and isotopic study. The samples dated are 1721025, 171026, 1721027 and 1721028 which are interpreted to have crystallisation ages of 3243 ± 4 Ma, 3252 ± 5 Ma, 1735 ± 6 Ma and 1733± 9 Ma, respectively. Samples 171025 and 171026 had new zircon growth at 2509 ± 4 Ma and 2507 ± 6 Ma, respectively. The young pink grained granite 1721027 and the mafic 1721028 have inherited zircon ages of up to ~3250 Ma and of ~2503 Ma (Jagodzinski, pers Comm. 2010).

Two periods of zircon growth (3242 ± 4 Ma and 2506 ± 6 Ma) are evident in sample 1721025. The sample is interpreted to have formed at 3242 Ma and then experienced a thermal event at 2506Ma, in which the metamorphic rims of the zircon formed and which caused the samples gneissic texture. The sample could also have been interpreted to have been formed at 2506Ma and to have inherited 3242Ma zircons. Zircon growth or disturbance caused by the Sleafordian, Cornian or Kimban orogenies is not shown within this sample (Jagodzinski, pers.Comm. 2010). Sample 1721026 is interpreted to have formed at 3252 ± 5 Ma with new zircon growth at 2507 ± 6 Ma. This sample could also have been interpreted to have been formed at 2507 ± 6Ma with 3252 ± 5 Ma inherited zircons. In summary, the SHRIMP U-Pb zircon data suggest the presence of crust as old as ~2342 Ma, which has undergone a thermal event at ~2510 Ma. The latter event produced both new zircon growth, Pb loss in older zircons and at least locally entirely new melts as evidenced by the ~2510 Ma Lake Giles Leucogranite dated by Fraser *et al.* (2010).

The gneissic granite samples 1721025 and 1721026 have been interpreted to be approximately 100 million years older than the 3150 Ma rocks identified by Fraser *et al.* (2010). The ages of these rock ages were both surprising and unsurprising. They were surprising in the sense that in the field and in hand specimen the rocks had been identified as the unnamed gneissic granite and the Cooyerdoo Granite, respectively, and were expected to have an age of ~3150Ma. However they were unsurprising in the sense that both ages had been identified by Fraser *et al.* (2010). Fraser *et al.* (2010)'s Cooyerdoo Granite, sample 2008371086, had inherited zircons ranging from ~3310 to 3215Ma, with one at 3240Ma, which indicated that there must been an older crust from which the zircons came. Fraser *et al.* (2010) had found both zircons within older granite and actual granites with the age ~2500Ma. The unnamed gneissic granite 2008371085 (3150Ma) had zircons with an age of ~2500Ma and the Lake Gilles Leucogranite (2008371081) is 2529Ma.

The younger granite and amphibolite samples 1721027 and 1721028, respectively, have inherited zircons going back to ~3250Ma and a population at ~2503Ma. The amphibolites and granitoids would have gained these inherited zircons by the melting of the older crust during their formation and accents (Jagodzinski, pers.Comm. 2010).

This study proposes that the Cooyerdoo and Unnamed Gneissic Granite are end members of the same unit and that the ~3240Ma granitoids (1721025 and 1721026), based on their similarity in appearance to the Cooyerdoo and Unnamed Gneissic Granite, could be part of the same tectonic event. This study does acknowledge that

even in geological time a 100 million year age gap is large but still think that these granites could be part of the same unit.

GEOCHEMICAL AND ISOTOPIC MTEHODS

Heat production measurements

Uranium, thorium and potassium measurements were taken in the field using a Radiation Solutions Inc. RS-230 BGO Super-Spec gramma ray spectrometer. It is a Bismuth-Germanium-oxide gamma ray spectrometer, which has a BGO detector crystal as opposed to other gamma ray spectrometers which tend to normally have a sodium-iodide detector. Measurements were taken by placing the gamma ray spectrometer against a rock and taking a reading. Readings were made on the freshest piece of rock available. Whole rock data for U, Th and P is also used in heat production calculations (see **whole rock geochemistry** for method).

Whole rock geochemistry

Samples had weathering removed and were crushed and milled using a tungsten mill. A proportion of milled sample was sent to the Amdel Laboratories, Adelaide, for major, trace and rare earth element analysis. A 0.1g proportion of the milled samples is fused with lithium metaborates and then dissolved in a nitric acid solution, which formed a ‘total solution’ which can be analysed by ICP-MS. Trace and REE elements are analysed by up to 0.5g of the sample being digested in HF-multi acid solutions, which put the sample in an liquid form that can then be analysed on the ICP-MS for specific elements (Payne *et al.* 2010).

Sm-Nd isotopes

Nd and Sm Isotopes were analysised at the University of Adelaide. A ^{150}Nd-^{147}Sm spike was used to spike the eight samples. The samples were evaporated in high pressure Teflon containers overnight and then hydrofluoric acid was added and the samples heated for 5 days at 190^{o}C in an oven. The samples were then evaporated to almost being dry and then HNO_3 was added and the samples were further evaporated. Hydrochloric acid was added and samples heated in the high-pressure Teflon containers for 2 days at 160^{o}C before being evaporated to dryness. The Nd and Sm were isolated by running the REE elements separate in HDEHP-impregnated Teflon powdered columns (Payne *et al.* 2010). The Finnigan MAT 262 Thermal Ionisation Mass Spectrometer TIMS was used to analyse both Nd and Sm isotopes. The standard GSP-2 had a measured ^{143}Nd-^{144}Nd value of 0.511397±0.000043 (1 st. dev., n = 5), and blanks was 600pg Nd. For Sm the standard GSP-2 had a measured ^{150}Sm-^{144}Sm value of 0.495798±0.000164 (1 st. dev., n = 3).

GEOCHEMICAL AND ISOTOPIC RESULTS

Major element geochemistry

The old granitoids are calc-alkaline to high-K calc alkaline (Figure 6) and have high silica (69.1-73.8 wt%) and Na_2O (3.61-5.15 wt%) and have low TiO_2 (0.11- 0.41 wt %), CaO (1.92-4.47 wt%), Fe_2O_3 (1.05-3 wt%) and MgO (0.24-0.96 wt %). The old granitoids plot in the granodiorite, trondhjemite and granite fields of the feldspar triangle (Figure 7). The old granitoids have Mg # (magnesium number) 31-40 young granites have Mg # of 12-28 (Table 2). The old granitoids are slightly peraluminous,

except 1721026 and 1723505 which are slightly metaluminous. They have an aluminium saturation index (ASI) of 0.99 to 1.06 and a Na_2O concentration 3.61 to 5.15 wt% (Table 2).

The younger granites are high-K calc-alkaline to slightly shoshonite (Figure 6) and have high silica (72.8-75.1 wt%) and Na_2O (3.25-4.37 wt%) and have low TiO_2 (0.13-0.24 wt %), CaO (0.6-1.32 wt%), Fe_2O_3 (0.43-1.69 wt%) and MgO (0.21-0.31 wt %). The young granites plot in the granite fields of the feldspar triangle (Figure 7). The young granites are slightly Peraluminous with an ASI of 1.01 to 1.07 and a Na_2O concentration of 3-4.37 wt%.

The amphibolites have mafic to intermediate silica (49.9-63.9 wt%) and varying MgO (1.39-8.28 wt%), TiO_2 (0.85-1.47 wt%), CaO (3.28-11.6 wt%) and Fe_2O_3 (5.26-15.2 wt%). On the mafic classification diagram (Figure 8) the amphibolites mainly plot as the intrusive version of basalt and they are mostly calc-alkaline while the young enriched amphibolites are shoshonite (Figure 6). The old amphibolites have Mg # 32-59, the young amphibolites have a Mg # 50-61.

Harker diagrams of the Mesoarchean and Paleoproterozoic granitoids suites are shown in Figure 9. Major oxides versus silica have been plotted and show that Al_2O_3, CaO, Fe_2O_3, MgO and P_2O_5 decrease with increasing silica, while Na_2O versus silica is very

scattered but appears to decrease with increasing silica content and as silica increases so does K_2O.

Trace and Rare Earth element geochemistry

Primitive mantle normalised trace element patterns for the old and young granite associations and the old and young mafic associations are shown in Figure 10. The old and young granitoids and the enriched amphibolites are enriched in the lighter trace and more depleted in the heavier trace elements. The older granites all have similar trace element patterns with Nb, P and Ti depletion. Sample 1721026 has a slightly different pattern with depleted Th compared to the enriched Th of the other samples. Samples of the younger granite association have a similar trace element pattern to the older granites with Nb, P and Yi. Sample 1723527 is depleted in Th while the other samples are enriched. The amphibolites follow the same trace element patterns as the granites but with a flatter trajectory and have higher heavy trace element concentrations than the old and young granitoids. The amphibolites appear to follow two different trace element pattern trends. The first is the enriched amphibolites with higher enrichment the elements Rb through to Eu and the second pattern has less enrichment. Both the young and old amphibolites have enriched and non-enriched amphibolites and the old amphibolites tend to plot at the bottom of both the enriched and non-enriched trends (Figure 10c). This overlap of depleted mantle patterns suggests that in some cases, amphibolites of the older and younger associations may have been incorrectly classified.

Chrondrite normalised rare earth element patterns, are shown in Figure 11. The ~3240Ma granites have positive or no Eu anomalies (0.9-4.57); while the ~3150 Cooyerdoo – unnamed gneiss granites have small negative Eu anomalies (0.64-1.04). Fraser et al 2010's Cooyerdoo and unnamed gneissic granites had small negative Eu anomalies (0.51-0.85). The young granite association have slight negative to no Eu anomalies (0.70-0.86). The amphibolites, once again, have two trends: an enriched light rare earth element trend and a less light rare earth element trend. The amphibolites all have no (or very small) Eu anomaly (0.9-1.01).

Sm-Nd Isotopes

The Sm-Nd isotopic results of 1721025, 1721026, 1721027, 1721028, 1723511, 1723516, 1723520 and 1723526 are in Table 3 and plotted on a neodymium evolution diagram (Figure 12), along with the Cooyerdoo Granite and unnamed gneissic granite neodymium data from Fraser *et al.* (2010). The ~3240Ma granitoids have ε_{Nd}(3240Ma) of 1.9 (sample 1721026) and 4.6 (sample 1721025) with depleted mantle model ages of 3277 Ma and 3143Ma. The older amphibolites have ε_{Nd} (3150Ma) of -0.4 and 3.26 with T_{DM} (depleted mantle model age) of 3320 and 3143 Ma. The younger granites and amphibolites plot close together with ε_{Nd} (1730Ma) ranging between -7.8 to -10.89 with T_{DM} of 2495 -2676Ma.

Heat production calculations

Surface heat productions for the Mesoarchean and Paleoproterozoic granitoid suites have been calculate from U, Th and K values calculated by the gamma ray spectrometer

(GRS) and whole rock geochemistry (Table 2). The whole rock surface heat production is potted against Th-U in Figure 13. Where both GRS data and whole rock data was obtained on the same rock samples the surface heat production were found to be very similar. The average surface heat production of the Cooyerdoo Granite and unnamed gneissic granite, at present age measured using the gamma ray spectrometer 2.93μW^{-3} and by whole rock geochemistry was 3.18 μW^{-3}. Fraser *et al.* (2010) has Cooyerdoo and unnamed gneissic granite have an average surface heat production of 4.71 μW^{-3}.The young granites only have whole rock geochemistry to calculate surface heat production and have an average surface heat production of 6.60 μW^{-3}. The old amphibolites (except the enriched 1723519) have a GRS surface heat production of 0.69 μW^{-3} (only one measurement was taken) and whole rock average surface heat production of 0.56 μW^{-3}. The enriched 1723519 has a surface heat production of 4.17 μW^{-3}. The enriched young amphibolites have a whole rock average surface heat production of 4.36 μW^{-3} and the one GRS analysis gave a surface heat production of 2.87 μW^{-3}. The non-enriched young amphibolites had an average GRS and surface heat production of 0.35 and 0.29 μW^{-3}, respectively.

DISCUSSION

This study has revealed more complexity within the eastern Gawler Craton, than identified in Fraser *et al.* (2010), which identified the presence of a Mesoarchean granitoid suite in the eastern Middleback Ranges and older ~3240 Ma inherited zircons within these rocks. A variation in geochemical and isotopic composition has been discovered, as opposed to the homogeneity of the suite in the Fraser *et al.* (2010) study.

All of the Fraser *et al.* (2010) data was collected in a small area, while the data of this study were collected over a larger area.

Source regions

Based on the similarity of the Cooyerdoo major and trace element composition with the potassic granites of the Yilgarn and Pilbara craton, Fraser *et al.* (2010) interpreted a similar origin for the Cooyerdoo Granite. Hence the Cooyerdoo could have been formed by the melting of an ~3400-3200Ma crust of with a Tonalite-Trondhjemite-Granodiorite, present below parts of the eastern Gawler Craton (Fraser *et al.* 2010).

Fraser *et al.* (2010) gave Sm-Nd isotopes data for four Cooyerdoo Granite and an unnamed gneissic granite samples. The samples had ε_{Nd} values of -0.9 to 1 and T_{DM} ages of 3280 to 3410 Ma indicative of the Cooyerdoo Granites's source region being an older 3280 to 3410 Ma crust. The ε_{Nd} of the Cooyerdoo Granite and unnamed gneissic granite (Fraser *et al.* 2010) plot away from the depleted mantle, which indicates they were formed by the recycling of older crust, as evidenced by the inherited zircons (between 3150Ma and ~3300Ma) found within the Cooyerdoo Granite. The ~3240Ma gneisses from this study have positive Eu values (2.06 and 4.60) and plot close to or slightly above the depleted mantle on a neodymium evolution diagram (Figure 12), indicating that they are very juvenile granites. This study has interpreted the Cooyerdoo and unnamed Gneissic Granites to be a part of the same granitoid suite as the ~3240Ma granitoids based on the similarity in their appearance and mineral assemblage. It is also

possible that the Cooyerdoo and unnamed Gneissic Granite formed from the ~3240Ma granitoids.

The gneissic granite samples (1721025 and 1721026), which were dated at 3243 and 3252 Ma, plot close to the depleted mantle curve. Sample 1721025 had ε_{Nd}(3243Ma) of 4.6 and a T_{DM} of 3143 Ma and sample 1721026 has ε_{Nd}(3252Ma) values of 1.9 and a T_{DM} of 3320 Ma. This would indicate that these granitoids are very juvenile and formed from the fractionation of a mantle derived magma source.

The two old amphibolites, 1723511 and 1723520, have ε_{Nd} (3150Ma) of -0.1 and 3.3 and T_{DM} values of 3320Ma and 3080Ma respectively and formed from a source that came from the mantle possibly during the same event as the ~3240 Ma granitoid and Cooyerdoo Granite forming event. The older amphibolite samples 1723511 and 1723519 are enriched in light rare earth and trace elements. These ε_{Nd} of the two older amphibolites are juvenile and may be reflecting a mantle enrichment that occurred during the 3240 Ma event.

Samples 1721025 and 1721026 have positive Eu anomalies, indicating that they were sourced from mantle where there is no plagioclase residue so no plagioclase to be removed from the source hence causing a positive Eu anomaly (Ragland 1989). The accumulation of feldspar or assimilation of materials rich in feldspar is indicated by a positive Eu anomaly (Ragland 1989). These granitoids are depleted in heavy rare earth elements, which indicates a juvenile mantle source.

The younger granites source regions is a crust somewhere around 2500 and 2600 Ma old, based on T_{DM} values from samples 1732516 and 1721027. Fraser *et al.* (2010) analysed a garnet leucogranite, west gillies that had an age of 1740 Ma, with an ε_{Nd} of -7.9 and a T_{DM} of 2700 Ma. These younger granites plot away from the depleted mantle and plot above or just on the Cooyerdoo Nd isotopic evolution field (Fig 12). The T_{DM} ages ~2500-2700Ma could possibly suggest that the younger granites were sourced from the re-working of a pre-existing ~2500-2600Ma crust. This pre-existing crust may be that identified in the zircon dating work as the thermal event at ~2510 Ma that. Only one sample of the young granite has been analysed for Nd-Sm but the remaining young granites are interpreted to have been formed from a source ~2500-2600Ma or older. It is possible that there are other young granites that formed from the ~3240-3150Ma granitoids.

The REE and primitive mantle plots of the older granites (except 1721025 and 1721026), which have not had geochronological data obtained, are very similar to those of Fraser *et al.* (2010) and for this reason these have been interpreted to be ~3150 Ma. To constrain further which age group these granites belong to further age dating and or Nd-Sm isotopic data needs to be performed.

The young amphibolites 1723526 and 1721028 are very enriched in trace elements, more so than the Cooyerdoo and young pink granite. Amphibolites can become enriched in trace elements via crustal contamination. Crustal contamination, however,

would also cause the amphibolites to become enriched in all of the the mineralogy of the granites (Tang *et al.* 2006). These amphibolites are still low in silica (52 and 59 wt% SiO2 respectively). Their ε_{Nd} values are very negative and formed from an enriched mantle source and this enrichment must have occurred along time ago.

Enrichment of mafic rocks can be caused by the mixing of mafic mantle and felsic granite but this would also increase the SiO_2. Sample 1723519 has a high silica content for an amphibolite so could conceivably be caused by the mixing of mantle and crust. The other samples, however, have silica contents that are much too low for mantle-crust mixing to be the cause. A possible cause of this enrichment is metasomatized lithospheric mantle, in which elements are preferentially added to the magma by enriched liquid coming off a subducting slab and then enriching the magma.

The enrichment of the amphibolite could be caused by crustal contamination, however this would produce an Eu anomaly and the enriched amphibolites in this study have no Eu anomalies. Therefore a metasomatized mantle is more likely to be the cause of the enrichment (Tang *et al.* 2006). The mixing of the depleted mantle and Fraser *et al.* (2010) is shown in figure 13 and a rock of the enrichment of the amphibolites cannot be formed by just mixing.

The amphibolite samples 1723515, 1723523, 1723528, 1723518 and 1723520 are much less enriched than the other amphibolites. This indicates that these amphibolite magma

did not come from an enriched mantle source and did not interact (mix or assimilate) with the crust and hence did not become enriched.

How could two sets of amphibolites rocks from the same area all not experience trace element enrichments? The mantle is heterogenous and the magmas of different enrichment may have been getting there source material from different areas of mantle with different enrichment levels. The enriched and non-enriched amphibolites were conceivably sampling different areas of the mantle but due to the close proximity of the sample locations the areas of mantle being sampled must still have been close together.

Tectonic setting of granites

The Archean was much hotter than the Earth is today with radiogenic heat production possibly four to six times higher (McKenzie & Weiss 1975). It was during the Archean that continental crust began to stabilise and it is debated whether (and in what form) plate tectonics operated in the Archean (Sleep & Windley 1982; Kroner 1985; Davies 1992; Condie 1997; Davies 1997; De Wit 1998). The heat would have been lost through processes at the Earth's surface caused by the mantle convections being increased. There would have been more tectonic activity (or Archean equivalent), such as greater magmatism and more heat transfer through the crust (Bickle 1978).

The old and young granitoids mostly plot within the volcanic arc granite and syn-collisonal granite field of the Nb versus Y diagram (Figure 14). On the Rb versus Y+Nb plot the young pink granites plot within the syn-collisonal granite field and the old granitoids just plot within the volcanic arc granite field (Figure 14). This would suggest a volcanic arc or syn-collisonal setting is possible; however this is only taking three very mobile elements (Rb, Y and Nb) in to account.

The old granitoids plot as granites, trondhjedmite and a granodiorite in a feldspar triangle (Figure 7) and are calc-alkaline, I type granites and are peraluminous to slightly metaluminous, while the young granites plots as granites on a feldspar triangle (Figure 7) and are calc-alkaline, I type granites and are peraluminous to slightly metaluminous. The old granitoids and young granites have been classified as I type granites because they have an ASI < 1.1 and have a Na2O concentration mostly above 3.2 wt % (Chappell & White 2001) and the old granitoids have hornblende which indicate they are metaluminous (Clarke 1992). The old granitoids have biotite and hornblende, while the young granite have biotite. Except for the granites being more granite than tonalite and granodiorite, they indicate a continental arc setting (Winter 2001).

The granites and amphibolites have depleted Nb and Ti, which is a feature that may suggest the granitoids formed in a convergent margin setting (Pearce & Peate 1995; Foley *et al.* 2002) since these depletions are typical of the continental crust (Rudnick & Gao 2003) and convergent margins are the site of much continental crust formation (Plank & Langmuir 1998; Barth *et al.* 2000). The primitive mantle diagrams from this study are similar to those of Swain *et al.* (2005), they both have the Nb and Ti depletion

and this indicates that the older and younger granites indicate a convergent margin environment.

The Archean Pilbara is thought to have formed in tectonic settings similar to tectonic settings that exist today, such as magmatic arc settings (Barley *et al.* 1998) and the accretion of island arc and continental fragments (Smith *et al.* 1998). At 3650 and 3150 Ma the Pilbara Craton experienced crustal growth (Smith *et al.* 1998).

Based on geochemistry, discrimination diagrams and depleted mantle plots a continental arc setting is inferred for both the younger and older associations.

Significance of older and younger associations

The older and younger associations are found in the same area and are hence sampling the same lithospheric region and may show changes in the lithosphere through time. The old ~3240Ma granitoids have a positive Eu anomaly, the Cooyerdoo-unnamed gneissic granite (~3150Ma) have a negative Eu anomaly while the young (~1745Ma) granites have a slight negative to no Eu anomaly (except the young granite sample 1723529 which has a positive Eu anomaly possibly due to alteration). The progression toward a negative Eu value indicates that the relationship of feldspar to the melt has changed from feldspar rich materials being accumulated and assimilated (positive Eu anomaly) to partial melting or feldspar fractionation (negative Eu anomaly). Europium anomalies only occurring in reducing magma environments so the lack of an Eu in the younger granite and amphibolites could indicate an oxidising magma environment, where Eu anomalies do not form (Ragland 1989).

The metasomatism of the mantle that caused the enriched younger amphibolites may have formed at a similar time as the ~3240 to 3150Ma crust. The enrichment is also present in some of the older amphibolites which indicates that there was already enrichment of the mantle in the Archean. The subduction in the Archean is a possible cause of the metasomatism and this would enrich both the older and younger amphibolites.

Heat production

For igneous lithologies a Th-U ration of four indicates primary magmatic Th-U. The Th-U ratios of the Mesoarchean and Palaeoproterozic granitoid suites mostly have primary Th-U, as shown in Figure 13 (Durrance 1986). This ratio will change if there is any secondary alteration, due to U and Th's variations in mobility (Neumann 2001).

The old and young granites and amphibolites have low surface heat production, much lower than the Burkitt Granite (Stewart, unpub data) of the eastern Eyre Peninsula (Figure 13). The average surface heat production of the older granitoids is 3.18 μWm^{-3} which is much lower than the average of those samples presented by Fraser *et al.* 2010 which was 4.7 μWm^{-3}. The ~3140Ma granitoids, the Cooyerdoo Granite and the ~1735 Ma granites (though these are higher than the older rocks) have low heat production. Fraser *et al.* (2010) used the SHRIMP to date the high Burkitt Granite at 1742 ± 42Ma which means that the high heat production has resided in 1742Ma granites and ~1590

Ma granitoids, such as the Charleston gneiss. The low heat production of the ~3240Ma granitoids or the Cooyerdoo Granite (or equivalent) are means it is unlikely they are the source of the SAHFA and that these high heat producing granitoids are formed from a different source. Magmatic reworking and crustal assimilation can enrich granitoids in heat producing elements. The high heat producing rocks, like the Hiltaba, hence cannot be formed simply by recycling older crust; instead they need a mantle input, and an enriched mantle input to account for the high heat flow.

The enriched young amphibolites have very high heat production values (and hence Th, U, K) of 3.22 and 5.53 μWm^{-1}, which are unusually high for mafic rocks which usually have low Th, U and K (Neumann 2001). These elements are more compatible with the crust than with the mantle and hence partition towards the crust, enriching the crust and depleting the mantle (Neumann 2001).These increased Th, U and K are caused by the metasomatized mantle.

CONCLUSIONS

The history of the Gawler Craton has been further extended with the identification of ~3240Ma rocks. An area of the Gawler Craton which had been once classified as the 'Lincoln complex', granites previously interpreted to be associated with the Paleoproterozoic, ~1730-1700 Ma Kimban Orogeny, has been found to be home of the oldest rocks in the Gawler Craton, with rocks of ~3150 Ma and ~3240 Ma now having been identified. These rocks may form the basement of the Galwer Craton or at least to the wedge shaped region defined by Fraser *et al.* (2010). Only two rocks have been

dated at ~3240Ma (SHRIMP) in the Gawler Craton so further rocks need to be analysed to determine the extent of these rock units. The amphibolites have been found to have both enriched and non-enriched compositions. The enrichment may have been formed by the metasomatism. The younger rocks follow similar trends to the older rocks and are interpreted to have evolved under a similar environment to the older rocks and using them as a source..Further work needs to be done on the enriched amphibolites to further understand the source of their enrichment. If plate tectonics existed during the Archean then a continental arc setting is suggested for the setting of the ~3240Ma granitoids and the Cooyerdoo granite. A continental arc setting is also inferred for the Paleoproterozoic granitoid suites.

ACKNOWLEDGMENTS

I would like to acknowledge and thank my supervisor Karin Barovich, Anthony Reid (PIRSA), Stacey McAvaney (PIRSA), Liz Jagodzinski (PIRSA), Fraser Farrell (who collected many of the samples) and Tony (Centrex), Centrex Metals Ltd and David Bruce.

REFERENCES

BARBARIN B. 1999. A review of the relationships between granitoid types, their origins and their geodynamnic environments. *Lithos* **46**, 605-626.

BARLEY M. E., LOADER S. E. & MCNAUGHTON N. J. 1998. 3420-3417 calc alkaline volcanism in the McPhee Dome and Kelly Belt, and growth of the eastern Pilbara Craton. *Precambrian Research* **88**, 3-23.

BARTH M. G., MCDONOUGH W. F. & RUDNICK R. L. 2000. Tracking the budget of Nb and Ta in the continental crust. *Chemical Geology* **165**, 197-213.

BICKLE M. J. 1978. Heat loss from the Earth: A constraint on Archaean tectonics from the relation between geothermal gradients and the rate of plate production. *Earth and Planetary Science Letters* **40**, 301-315.

BONIN B. 1990. From orogenic to anorogenic settings: evolution of granitoid suites after a major orogenesis. *Geological Journal* **25**, 261-270.

CHAPPELL B. W. & WHITE A. J. R. 2001. Two contrasting granite types: 25 years later. *Australian Journal of Earth Sciences* **48**, 489-499.

CLARKE D. B. 1992. *Granitoid rocks.* Chapman and Hall, London.

CLEMENS J. D., YEARRON L. M. & STEVENS G. 2006. Barberton (SOuth Africs) TTG magmas: Geochemical and experimental constraints on source-rock petrology, pressure of formation and tectonic setting. *Precambrian Research* **151**, 53-78.

CONDIE K. C. 1993. Chemical composition and evolution of the upper continental crust: Contrasting results from surface samples and shales. *Chemical Geology* **104**, 1-37.

CONDIE K. C. 1997. *Plate Tectonics and Crustal Evolution.* Butterworth-Heinemann, London.

CREASER R. A. & FANNING C. M. 1993. A U-Pb zircon study of the Mesoproterozoic Charleston Granite, Gawler Craton, South Australia. *Australian Journal of Earth Sciences* **40**, 519-526.

DALY S. J. & FANNING C. M. 1993. *Archaean. In: Dexel,J.F., W.V.,Parker, A.J.(Eds.).The Geology of South Australia, vol.1* (The Precambrian. Geological Survey of South Australia, Bulletin 54).

DAVIES G. F. 1992. On the emergence of plate tectonics. *Geology* **20**, 963-966.

DAVIES G. F. 1997. the mantle dynamical repertoire: plates, plumes, overtunrs and tectonic evolution. *AGSO Journal of Australian Geology & Geophysics* **17**, 93-99.

DE S. K., CHACKO T., CREASER R. A. & MUEHLENBACHS K. 2000. Geochemical and Nd-Pb-O isotope systematics of granites from the Taltson Magmatic Zone, NE Alberta: implications for early Proterozoic tectonics in western Laurentia. *Precambrian Research* **102**, 221-249.

DE WIT M. 1998. On Archaean granites, greenstones, cratons, and tectonics: does the evidence demand a verdict? *Precambrian Research* **91**, 181-226.

DURRANCE E. M. 1986. *Radioactive in Geology; Principles and applications.* Ellis Horwood Limited, West Sussex.

EKLUND O., KONOPELKO D., RUTANEN H., FROJDO S. & SHEBANOV A. D. 1998. 1.8 Ga Svecofennian post-collisional shoshonitic magmatism in the Fennoscandian shield. *Lithos* **45**, 87-108.

FODEN J., BUICK I. S. & MORTIMER G. E. 1988. The petrology and geochemistry of granitic gneisses from the east Arunta Inlier, central Australia: implications for Proterozoic crustal development. *Precambrian Research* **40/41**, 233-259.

FOLEY S., TIEPLOL M. & VANNUCCI R. 2002. Growth of early continental crust controlled by melting of amphibolite in subduction zones. *Nature* **417**, 837-840.

FRASER G., MCAVANEY S., NEUMANN N., SZPUNAR M. & REID A. 2010. Discovery of early Mesoarchean crust in the eastern Gawler Craton, South Australia. *Precambrian Research* **in press**.

FROST B. R., BARNES C. G., COLLINS W. J., ARCULUS R. J., ELLIS D. J. & FROST C. D. 2001. A Geochemical Classification for Granitic Rocks. *Journal of Petrology* **42**, 2033-2048.

GLIKSON A. Y. 1979. Early Precambrian Tonalite-Trondhjemite Sialic Nucleu. *Earth Science Reviews* **15**, 1-73.

HAND M., REID A. & JAGODZINSKI L. 2007. Tectonic Framework and Evolution of the Gawler Craton, Southern Australia. *Economic Geology* **102**, 1377-1395.

KRONER A. 1985. Evolution of the Archean continental crust. *Annual Review of Earth and Planetary Sciences* **13**, 49-74.

MANIAR P. D. & PICCOLI P. M. 1989. Tectonic discrimination of granitoids. *Geological Society of America Bulletin* **101**, 635-643.

MARTIN H. 1994. *The Archean grey gneisses and genis of continetal crust. In: Condie, K.C. (Ed.), Archean Crustal Evolution, Devlopments in Precambrain Geology* (Vol. 11). Elsevier, Amsterdam.

MCKENZIE D. & WEISS N. 1975. Spectulations on the thermal and tectonic history of the Earth. *Geophysical Journal of the Royal Astronomical Society* **42**, 31-174.

NEUMANN N. 2001. Geochemical and isootopic characteristics of South Australian Proterozoic granites: Implications for the origin and evolution of high heat-producing terrains. Department of Geology and Geophysics, The Univeristy of Adelaide, Adelaide (unpubl.).

NEUMANN N., SANDIFORD M. & FODEN J. 2000. Regional geochemistry and continetal heat flow: implications for the origin of the South Australia heat flow anomaly. *Earth and Planetary Science Letters* **183**, 107-120.

PARKER A. J. (Editor) 1980. *The Kalinjala mylonite zone, eastern Eyre Peninsula A.J. eds. the Geology of South Australia Volume 1: The Precambrian, pp. 71-81*. Geological Survey of South Australia, Adelaide.

PARKER A. J. 1993. Geological Framework. In: Drexel., F.J, Preiss, W.V. and Parker, A.J. (eds.) The Geology of South Australia. Volume I. The Precambrian. *Geological Survey of South Australia* **54**, 8-31.

PAUL E., FLOTTMANN T. & SANDIFORD M. 1999. Structural geometry and controls on basement-involved deformation in the northern Flinders Ranges, Adelaide Fold Belt, South Australia. *Australian Journal of Earth Sciences* **46**, 343-354.

PAYNE J. L., FERRIS G., BAROVICH K. M. & HAND M. 2010. Pitfalls of classifying ancient magmatic suites with tectonic discrimination diagrams: An example from the Paleoproterozoic Tunkillia Suite, southern Australia. *Precambrian Research* **177**.

PEARCE J. A. & PEATE D. W. 1995. Tectonic implication of the composition of volcanic arc magmas. *Annual Review of Earth and Planetary Sciences* **23**, 251-281.

PETERSON T., VAN BREEMEN O., SANDEMAN H. & COUSENS B. 2002. Proterozoic (1.85-1.75 Ga) igneous suites of the Western Churchill Province: granitoid and ultrapotassic magmatism in a reworked Archean hinterland. *Precambrian Research* **119**, 73-100.

PETFORD N., CLEMENS J. D. & VIGNERESSE J. L. 1997. Application of infromation theory to the formation of granitic rocks. *In* Bouchez, J.L., Hutton, D. & Stephens, W.E. (eds) *Granite from Melt Segregation to Emplacement Fabrics,* 3-10. Dordrecht: Kluwer Academic Publishers.

PLANK T. & LANGMUIR C. H. 1998. The chemical composition of subducting sediments and its consequence for the crust and mantle. *Chemical Geology* **145**, 325-394.

RAGLAND P. C. 1989. *Basic Analytical Petrology.* Oxford University Press, Oxford.

REID A. J., FLINT R., ROLAND M., HOWARD K. E. & BELOUSOVA E. A. 2009. Geochronological and isotopic constraints on Palaeoproterozoic skarn base metal mineralisation in the central Gawler Craton, South Australia. *Ore Geology Reviews* **36**, 350-362.

REID A. J., HAND M., JAGODZINSKI E., KELSEY D. E. & PEARSON N. 2008. Paleoproterozoic orogenesis in the southeastern Gawler Craton, south australia. *Australian Journal of Earth Sciences* **55**, 449-444.

RUDNICK R. L. & GAO S. 2003. Composition of the Continental Crust. *In:* Heinrich D. H. & Karl K. T. eds., *Treatise on Geochemistry*, pp 1-64, Pergamon, Oxford.

SCHAEFER B. F. 1998. Insights into Proterozoic tectonics from the southern Eyre Peninsula, South Australia. Department of Geology and Geophysics, The University of Adelaide, Adelaide (unpubl.).

SLEEP N. H. & WINDLEY B. F. 1982. Archean plate tectonics: constraints and inferences. *Journal of Geology* **90**, 363-379.

SMITH J. B., BARLEY M. E., GROVES D. I., KRAPEZ B., MCNAUGHTON N. J., BICKLE M. J. & CHAPMAN H. J. 1998. The Sholl Shear Zone, West Pilbara; evidnece for a domain boundary structure from integrated tectonostratigraphic analyses, SHRIMP U-Pb dating and isotopic and geochemical data of granitoids. *Precambrian Research* **88**, 143-171.

SUN S. & MCDONOUGH W. F. 1989. Chemical and isotopic systematics of oceanic basalts; implications for mantle composition and processes. In: Saunders, A.D., Norry, M.J. (eds.), Magmatism in the oceanic basins. *Geological Society of London*, 313-345.

SWAIN G., HAND M., TEASDALE J., L R. & CLARK C. 2005a. Age constraints on terrane-scale shear zones in the Gawler Craton, southern Australia. *Precambrian Research* **139**, 164-180.

SWAIN G., WOODHOUSE A., HAND M., BAROVICH K. M., SCHWARZ M. & FANNING C. M. 2005b. Provenance and tectonic development of the late Archean Gawler Craton, Australia; U-Pb zircon, geochemical and Sm-Nd isotopic implications. *Precambrian Research* **141**, 106-136.

TANG Y.-J., ZHANG H.-F. & YING J.-F. 2006. Asthenosphere-lithosphere mantle interaction in an extensional regime: Implication from the geochemistry of Cenozoic basalts from Taihang Mountains, North China craton. *Chemical Geology* **233**, 309-327.

VASSALLO J. J. & WILSON C. J. L. 2002. Palaeoproterozoic regional-scale non-coaxial deformation: an example from eastern eyre Peninsula, South Australia. *Journal of Structural Geology* **24**, 1-24.

VIGNERESSE J. L. 2004. A new paradigm for granite generation. *Transactions of the Royal Society of Edinburgh: Earth Scrience* **95**, 11-22.

WHALEN J. B., PERCIVAL J. A., MCNICOLL V. J. & LONGSTAFFE F. 2004. Geochemical and isotopic (Nd-O) evidence bearing on the origin of late- to post-orogenic high-K granitoid rocks in the Western Superior Province: implications for late Archean tectonomagmatic processes. *Precambrian Research* **132**, 303-326.

WINTER J. D. 2001. *An introduction to Igneous and Metamorphic Petrology* (second edition). Prentice Hall, New Jersey.

YANG J., CHUNG S., ZHAI M. & ZHOU X. 2004. Geochemical and Sr-Nd-Pb isotopic compositions of mafic dikes from the Jiaodong Peninsula, China: evidence for vein-plus-peridotite melting in the lithospheric mantle. *Lithos* **73**, 145-160.

YEATES G. 1990. *Yeates, G., 1990. Middleback Range iron ore deposits. In: F.E. Hughes (Editor), Geology of the mineral deposits of Australia and Papua New Guinea; Volume 2. Monograph Series - Australasian Institute of Mining and Metallurgy. Australasian Institute of Mining and Metallurgy, Melbourne, Victoria, Australia.* Monograph series.

LIST OF TABLES

LIST OF FIGURES

Figure 4 Photographs of a) Cooyerdoo Granite (1723505), b) young pink granite (1723530), c) segregation in unnamed gneissic granite (1723513), c) mylonite zone with unnamed gneissic granite and mafic (1723521), e) young mafic (1723528) f) enriched young mafic (1723526),

Figure 5 Characteristic thin sections of a) ~3240Ma granitoids (sample 1721025), b) young pink granite (sample 1721027), c) young mafic (sample 1721028) and d) old mafic (sample 1723511), in the eastern Gawler Craton. Photos are under plain and cross-polarised light of the same image.

Figure 6 The amount of K_2O in relationship to SiO_2 is shown for the Mesoarchean and Paleoproterozoic granitoids and amphibolites from the eastern Eyre Peninsula. The level of potassium field are from Peccerillo and Taylor (1976).

Figure 7 CIPW normative An-An-Or classification after O'Connor 1965 of the Mesoarchean Granitoids, eastern Eyre Peninsula.

Figure 8 A classification plot for mafic rocks showing where the Mesoarchean and Paleoproterozoic amphibolites plot. The rocks in this study are the intrusive equivalent to the mafics.

Figure 9 Harker diagrams for the Mesoarchean and Paleoproterozoic Granitoids and Amphibolites, eastern Eyre Peninsula

Figure 10 Primitive normalised (Sun & McDonough 1989) mantle plots a) old granitoids (~3240Ma granitoids have the open squares and are red, while the ~3150Ma granitoids have the filled in squares and are brown-red) b) young granites c) Fraser data d) old mafics (green) and young mafics (blue).

Figure 11 Chrondrite-normalised (Boynton 1984) rare-earth element plots a) old granites (~3240Ma granitoids have the open squares and are red, while the ~3150Ma granitoids have the filled in squares and are brown-red) b) young granites c) Fraser et al C) old mafic (green) and young mafics (blue).

Figure 12 Mesoarchean and Paleoproterozoic granitoids and amphibolites plotted on a neodymium evolution diagram. The grey represents the Nd-isotopic composition of the Cooyerdoo Granite and unnamed gneissic granite from Fraser *et al.* (2010).

Figure 13: The blue lines with triangles are the enriched mafics and the green lines are the possible geochemistry of a rock formed from the mixing of the cooyerdoo (2008371086) (Fraser et al 2010) and a depleted mantle (Workman & Hart 2004).

Figure 14 Log-log plots of a) Rb vs. Y + Nb and b) Nb vs. Y (in ppm), with tectonic a settings from Pearce *et al.* (1984).

Figure 15 Surface heat production versus Th/U of the Meosarchean and Paleoproterozoic Granitoid Suites and the Burkitt Granite (Stewart unpub data), in the eastern Eyre Peninsula.

TABLES

Table 1

Unit	Age (Ma)	Source of Age	Minerals	texture
~3240 Ma Granitoids	3240	Jagodzinski, PIRSA, pers. Comm. 2010	Quartz, plagioclase, k-feldspar and biotite ± hornblende	Gneissic
Cooyerdoo Granite	3150	Fraser *et al.* 2010	Quartz, plagioclase and biotite ± hornblende	Gneissic
Unnamed Gneissic Granite	3150	Fraser et al. 2010	Quartz, plagioclase, k-feldspar and biotite	Gneissic
Young Pink Granite	1735	Jagodzinski, PIRSA, pers. Comm. 2010	Quartz, k-feldspar and plagioclase	Granitic
Old Amphibolite	3150	Based on proximity to ~3150 Ma granitoids	Hornblende, plagioclase, clinopyroxene	Foliated
Young Enriched Amphibolite	3150	Jagodzinski, PIRSA, pers. Comm. 2010	Hornblende and plagioclase	Foliated
Young Amphibolite	1735	Based on proximity to ~1630 Ma granitoids	Plagioclase, hornblende, quartz	

Table 2

IDENT		1723518	1723519	1723520	1723516	1723517	1721027	1723515	1723523	1723528	1723526	1721028
rock type		amphibolite	amphibolite	amphibolite	granite	granite	granite	amphibolite	amphibolite	amphibolite	amphibolite	amphibolite
age		~3150	~3150	~3150	~3150	~3150	1735	~1730	~1730	~1730	~1730	1733
E(53)		693969	693998	693886	691694	691670	691278	691315	690167	691510	693824	690177
N(53)		6314663	6314650	6314693	6312302	6312337	6317937	6312619	6319084	6317886	6313228	6319074
Al2O3	%	14.7	15.9	13.9	13.8	14.2	13.9	12.4	10.8	15.1	14.5	14.1
CaO	%	10.1	3.3	9.3	0.7	1.0	0.6	9.2	9.0	11.1	5.7	5.5
Fe2O3	%	11.5	5.8	12.0	1.3	1.7	1.1	15.2	14.5	11.4	8.7	5.3
K2O	%	1.4	2.5	1.1	5.3	5.8	4.9	1.1	0.9	0.6	4.7	5.4
MnO	%	0.2	0.1	0.2	0.0	0.0	0.0	0.2	0.2	0.2	0.1	0.1
MgO	%	7.8	1.4	7.2	0.2	0.3	0.2	7.0	7.5	6.8	5.0	4.2
Na2O	%	2.4	4.9	3.0	3.8	3.5	3.9	2.5	2.5	2.3	3.5	3.4
P2O5	%	0.1	0.4	0.1	0.0	0.0	0.1	0.1	0.1	0.1	0.8	0.8
SiO2	%	50.1	63.9	51.8	73.1	72.8	73.6	49.9	51.5	50.5	52.4	59.0
TiO2	%	0.9	0.9	0.9	0.1	0.2	0.1	1.0	1.3	0.9	1.4	1.0
LOI	%	1.8	0.6	1.4	0.6	0.5	1.5	1.0	1.3	0.9	1.3	1.0
Cr	ppm	300.0	20.0	95.0	<20	<20	<20	125.0	460.0	160.0	145.0	145.0
V	ppm	285.0	90.0	290.0	<20	<20	<20	345.0	320.0	275.0	140.0	110.0
Sc	ppm	40.0	<5	40.0	<5	<5	<5	45.0	30.0	40.0	20.0	15.0
U	ppm	<0.5	3.0	0.5	7.5	12.5	10.5	0.5	0.5	0.5	3.5	6.5
Th	ppm	0.5	46.5	1.0	60.0	80.0	44.5	2.0	2.5	0.5	28.5	50.0
Mo	ppm	<2	<2	<2	<2	<2	<2	<2	<2	<2	<2	<2
Rb	ppm	75.0	75.0	47.5	235.0	280.0	250.0	35.0	41.5	25.0	100.0	155.0
Sr	ppm	315.0	1000.0	205.0	230.0	190.0	395.0	200.0	310.0	155.0	1200.0	1200.0
Ba	ppm	295.0	1100.0	235.0	950.0	900.0	1000.0	650.0	230.0	180.0	6200.0	4000.0
Be	ppm	<0.5	1.0	<0.5	3.5	2.5	6.5	<0.5	1.0	4.0	4.0	7.0
Ce	ppm	18.0	325.0	18.0	110.0	185.0	80.0	23.0	32.0	13.0	420.0	240.0
La	ppm	7.0	180.0	8.0	65.0	110.0	43.0	12.0	14.0	5.0	185.0	100.0
Hf	ppm	1.0	7.0	2.0	4.0	5.0	4.0	2.0	3.0	1.0	9.0	8.0
Y	ppm	16.0	17.0	20.0	5.0	7.0	8.0	26.0	22.0	20.0	24.0	18.0
Ag	ppm	0.2	<0.1	<0.1	<0.1	<0.1	<0.1	<0.1	0.1	<0.1	0.1	<0.1
As	ppm	1.5	1.0	2.5	1.5	1.0	1.0	1.5	1.0	<0.5	1.5	2.0
Bi	ppm	0.2	<0.1	0.3	0.1	<0.1	<0.1	0.1	0.2	<0.1	0.2	<0.1
Cd	ppm	0.1	<0.1	<0.1	<0.1	<0.1	<0.1	<0.1	<0.1	<0.1	<0.1	<0.1
Co	ppm	55.0	32.0	60.0	65.0	60.0	30.5	60.0	65.0	48.5	45.5	32.0
Cs	ppm	2.3	0.9	2.6	2.1	1.8	1.9	0.8	0.7	1.2	1.4	0.4
Cu	ppm	85.0	21.5	105.0	1.5	<0.5	3.0	75.0	165.0	85.0	30.0	17.0
Ga	ppm	16.5	26.5	17.5	26.5	29.5	28.0	19.0	21.0	19.0	26.5	24.5
In	ppm	<0.5	<0.5	<0.5	<0.5	<0.5	<0.5	<0.5	<0.5	<0.5	<0.5	<0.5
Ni	ppm	75.0	12.0	45.0	2.0	<2	7.0	85.0	165.0	60.0	90.0	85.0
Pb	ppm	8.5	23.5	11.5	50.0	70.0	32.5	12.0	20.0	7.5	27.0	22.0
Sb	ppm	<0.5	<0.5	<0.5	<0.5	<0.5	<0.5	<0.5	<0.5	<0.5	<0.5	<0.5
Se	ppm	<0.5	<0.5	<0.5	<0.5	<0.5	<0.5	<0.5	<0.5	<0.5	<0.5	<0.5
Te	ppm	<0.2	<0.2	<0.2	<0.2	<0.2	<0.2	<0.2	<0.2	<0.2	<0.2	<0.2
Tl	ppm	0.5	0.5	0.3	1.2	1.5	1.3	0.3	0.3	0.2	0.9	0.9
Zn	ppm	115.0	115.0	115.0	24.0	34.0	16.5	130.0	125.0	95.0	100.0	65.0
Dy	ppm	3.6	3.3	4.0	0.9	1.8	1.2	5.5	5.5	4.2	6.5	4.8
Er	ppm	2.1	1.8	2.6	0.5	0.8	0.7	3.4	2.7	2.7	2.6	2.0
Eu	ppm	1.2	2.2	1.1	0.6	1.2	0.6	1.3	1.8	1.1	6.5	4.7
Gd	ppm	3.6	5.5	3.7	1.6	3.4	1.8	4.9	6.0	3.8	14.5	10.5
Ho	ppm	0.8	0.6	0.9	0.2	0.3	0.2	1.2	1.1	0.9	1.1	0.8
Lu	ppm	0.3	0.2	0.3	0.1	0.1	0.1	0.5	0.3	0.4	0.3	0.2
Nd	ppm	13.5	85.0	12.0	24.0	60.0	25.5	16.5	23.5	10.5	215.0	140.0
Pr	ppm	3.2	27.0	2.6	8.0	20.5	8.0	3.9	5.5	2.2	60.0	37.0
Sm	ppm	3.1	9.5	3.0	3.2	7.5	3.2	4.0	5.5	2.9	29.0	19.5
Tb	ppm	0.6	0.7	0.6	0.2	0.4	0.2	0.9	0.9	0.7	1.6	1.2
Tm	ppm	0.3	0.2	0.4	0.1	0.1	0.1	0.5	0.4	0.4	0.3	0.3
Yb	ppm	2.0	1.4	2.4	0.5	0.6	0.7	3.3	2.3	2.5	2.0	1.6
Nb	ppm	3.0	14.0	2.0	7.0	10.0	14.0	3.0	3.0	2.0	23.0	12.0
Zr	ppm	55.0	320.0	55.0	140.0	190.0	115.0	75.0	105.0	50.0	415.0	370.0
Eu/Eu*		1.1	0.9	1.0	0.9	0.7	0.8	0.9	1.0	1.0	1.0	1.0
ASI =A/CNK					1.0	1.0	1.1					
K (GRS)	%				2.3				0.4	1.7	3.1	
U (GRS)	ppm				0.7				0.0	1.0	2.5	
Th (GRS)	ppm				31.7				2.8	1.0	28.2	
heat production (GRS)	μW^{-3}								0.2	0.5	2.9	
heat production (geochem)	(μW^{-3})		4.0	0.2	6.1	8.7	5.8	0.3	0.3	0.2	2.9	5.1
Th/U (geochem)			15.5	2.0	8.0	6.4	4.2	4.0	5.0	1.0	8.1	7.7

Table 2 (cont.)

IDENT		1723518	1723519	1723520	1723516	1723517	1721027	1723515	1723523	1723528	1723526	1721028
rock type		amphibolite	amphibolite	amphibolite	granite	granite	granite	amphibolite	amphibolite	amphibolite	amphibolite	amphibolite
age		~3150	~3150	~3150	~3150	~3150	1735	~1730	~1730	~1730	~1730	1733
E(53)		693969	693998	693886	691694	691670	691278	691315	690167	691510	693824	690177
N(53)		6314663	6314650	6314693	6312302	6312337	6317937	6312619	6319084	6317886	6313228	6319074
Al2O3	%	14.7	15.9	13.9	13.8	14.2	13.9	12.4	10.8	15.1	14.5	14.1
CaO	%	10.1	3.3	9.3	0.7	1.0	0.6	9.2	9.0	11.1	5.7	5.5
Fe2O3	%	11.5	5.8	12.0	1.3	1.7	1.1	15.2	14.5	11.4	8.7	5.3
K2O	%	1.4	2.5	1.1	5.3	5.8	4.9	1.1	0.9	0.6	4.7	5.4
MnO	%	0.2	0.1	0.2	0.0	0.0	0.0	0.2	0.2	0.2	0.1	0.1
MgO	%	7.8	1.4	7.2	0.2	0.3	0.2	7.0	7.5	6.8	5.0	4.2
Na2O	%	2.4	4.9	3.0	3.8	3.5	3.9	2.5	2.5	2.3	3.5	3.4
P2O5	%	0.1	0.4	0.1	0.0	0.0	0.1	0.1	0.1	0.1	0.8	0.8
SiO2	%	50.1	63.9	51.8	73.1	72.8	73.6	49.9	51.5	50.5	52.4	59.0
TiO2	%	0.9	0.9	0.9	0.1	0.2	0.1	1.0	1.3	0.9	1.4	1.0
LOI	%	1.8	0.6	1.4	0.6	0.5	1.5	1.0	1.3	0.9	1.3	1.0
Cr	ppm	300.0	20.0	95.0	<20	<20	<20	125.0	460.0	160.0	145.0	145.0
V	ppm	285.0	90.0	290.0	<20	<20	<20	345.0	320.0	275.0	140.0	110.0
Sc	ppm	40.0	<5	40.0	<5	<5	<5	45.0	30.0	40.0	20.0	15.0
U	ppm	<0.5	3.0	0.5	7.5	12.5	10.5	0.5	0.5	0.5	3.5	6.5
Th	ppm	0.5	46.5	1.0	60.0	80.0	44.5	2.0	2.5	0.5	28.5	50.0
Mo	ppm	<2	<2	<2	<2	<2	<2	<2	<2	<2	<2	<2
Rb	ppm	75.0	75.0	47.5	235.0	280.0	250.0	35.0	41.5	25.0	100.0	155.0
Sr	ppm	315.0	1000.0	205.0	230.0	190.0	395.0	200.0	310.0	155.0	1200.0	1200.0
Ba	ppm	295.0	1100.0	235.0	950.0	900.0	1000.0	650.0	230.0	180.0	6200.0	4000.0
Be	ppm	<0.5	1.0	<0.5	3.5	2.5	6.5	<0.5	1.0	4.0	4.0	7.0
Ce	ppm	18.0	325.0	18.0	110.0	185.0	80.0	23.0	32.0	13.0	420.0	240.0
La	ppm	7.0	180.0	8.0	65.0	110.0	43.0	12.0	14.0	5.0	185.0	100.0
Hf	ppm	1.0	7.0	2.0	4.0	5.0	4.0	2.0	3.0	1.0	9.0	8.0
Y	ppm	16.0	17.0	20.0	5.0	7.0	8.0	26.0	22.0	20.0	24.0	18.0
Ag	ppm	0.2	<0.1	<0.1	<0.1	<0.1	<0.1	<0.1	0.1	<0.1	0.1	<0.1
As	ppm	1.5	1.0	2.5	1.5	1.0	1.0	1.5	1.0	<0.5	1.5	2.0
Bi	ppm	0.2	<0.1	0.3	0.1	<0.1	<0.1	0.1	0.2	<0.1	0.2	<0.1
Cd	ppm	0.1	<0.1	<0.1	<0.1	<0.1	<0.1	<0.1	<0.1	<0.1	<0.1	<0.1
Co	ppm	55.0	32.0	60.0	65.0	60.0	30.5	60.0	65.0	48.5	45.5	32.0
Cs	ppm	2.3	0.9	2.6	2.1	1.8	1.9	0.8	0.7	1.2	1.4	0.4
Cu	ppm	85.0	21.5	105.0	1.5	<0.5	3.0	75.0	165.0	85.0	30.0	17.0
Ga	ppm	16.5	26.5	17.5	26.5	29.5	28.0	19.0	21.0	19.0	26.5	24.5
In	ppm	<0.5	<0.5	<0.5	<0.5	<0.5	<0.5	<0.5	<0.5	<0.5	<0.5	<0.5
Ni	ppm	75.0	12.0	45.0	2.0	<2	7.0	85.0	165.0	60.0	90.0	85.0
Pb	ppm	8.5	23.5	11.5	50.0	70.0	32.5	12.0	20.0	7.5	27.0	22.0
Sb	ppm	<0.5	<0.5	<0.5	<0.5	<0.5	<0.5	<0.5	<0.5	<0.5	<0.5	<0.5
Se	ppm	<0.5	<0.5	<0.5	<0.5	<0.5	<0.5	<0.5	<0.5	<0.5	<0.5	<0.5
Te	ppm	<0.2	<0.2	<0.2	<0.2	<0.2	<0.2	<0.2	<0.2	<0.2	<0.2	<0.2
Tl	ppm	0.5	0.5	0.3	1.2	1.5	1.3	0.3	0.3	0.2	0.9	0.9
Zn	ppm	115.0	115.0	115.0	24.0	34.0	16.5	130.0	125.0	95.0	100.0	65.0
Dy	ppm	3.6	3.3	4.0	0.9	1.8	1.2	5.5	5.5	4.2	6.5	4.8
Er	ppm	2.1	1.8	2.6	0.5	0.8	0.7	3.4	2.7	2.7	2.6	2.0
Eu	ppm	1.2	2.2	1.1	0.6	1.2	0.6	1.3	1.8	1.1	6.5	4.7
Gd	ppm	3.6	5.5	3.7	1.6	3.4	1.8	4.9	6.0	3.8	14.5	10.5
Ho	ppm	0.8	0.6	0.9	0.2	0.3	0.2	1.2	1.1	0.9	1.1	0.8
Lu	ppm	0.3	0.2	0.3	0.1	0.1	0.1	0.5	0.3	0.4	0.3	0.2
Nd	ppm	13.5	85.0	12.0	24.0	60.0	25.5	16.5	23.5	10.5	215.0	140.0
Pr	ppm	3.2	27.0	2.6	8.0	20.5	8.0	3.9	5.5	2.2	60.0	37.0
Sm	ppm	3.1	9.5	3.0	3.2	7.5	3.2	4.0	5.5	2.9	29.0	19.5
Tb	ppm	0.6	0.7	0.6	0.2	0.4	0.2	0.9	0.9	0.7	1.6	1.2
Tm	ppm	0.3	0.2	0.4	0.1	0.1	0.1	0.5	0.4	0.4	0.3	0.3
Yb	ppm	2.0	1.4	2.4	0.5	0.6	0.7	3.3	2.3	2.5	2.0	1.6
Nb	ppm	3.0	14.0	2.0	7.0	10.0	14.0	3.0	3.0	2.0	23.0	12.0
Zr	ppm	55.0	320.0	55.0	140.0	190.0	115.0	75.0	105.0	50.0	415.0	370.0
Eu/Eu*		1.1	0.9	1.0	0.9	0.7	0.8	0.9	1.0	1.0	1.0	1.0
ASI =A/CNK					1.0	1.0	1.1					
K (GRS)	%				2.3				0.4	1.7	3.1	
U (GRS)	ppm				0.7				0.0	1.0	2.5	
Th (GRS)	ppm				31.7				2.8	1.0	28.2	
heat production (GRS)	μW^{-3}								0.2	0.5	2.9	
heat production (geochem)	(μW^{-3})		4.0	0.2	6.1	8.7	5.8	0.3	0.3	0.2	2.9	5.1
Th/U (geochem)			15.5	2.0	8.0	6.4	4.2	4.0	5.0	1.0	8.1	7.7

Table 3

Sample number	Rock type	Sm ppm	Nd ppm	147Sm/144Nd	143Nd/144Nd	Age (Ma)	εNd(o)	$\varepsilon_{Nd\,(T)}$	TDM (Ma)
1721026	Gneiss Granite	1.86	13.82	0.0814	0.510266	3252	-46.2	2.06	3116
1721028	Amphibolite	15.59	111.37	0.0846	0.51091	1733	-33.7	-8.86	2615
1723516	Granite	3.64	29.24	0.0753	0.51086	1730	-34.6	-7.80	2495
1723511	Amphibolite	11.72	82.74	0.0857	0.510322	3150	-45.1	-0.14	3320
1723526	Amphibolite	22.69	175.03	0.0784	0.510846	1730	-34.9	-8.75	2566
1723520	Amphibolite	2.41	9.37	0.1557	0.511953	3150	-13.3	3.26	3082
1721025	Gneiss Granite	2.11	23.17	0.0553	0.509843	3243	-54.5	4.60	3143
1721027	Granite	2.97	23.41	0.0769	0.51072	1735	-37.4	-10.89	2676

FIGURES

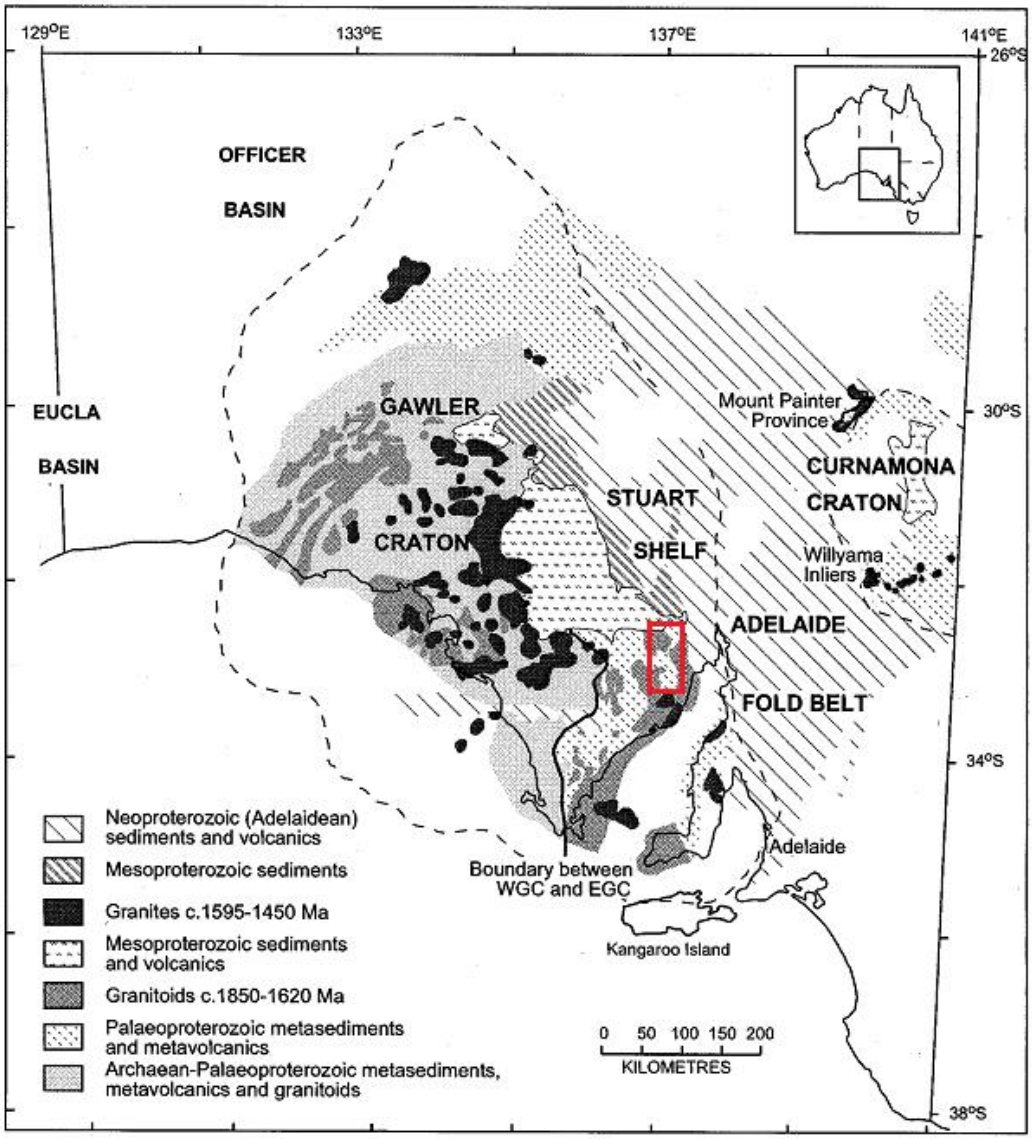

Figure 1

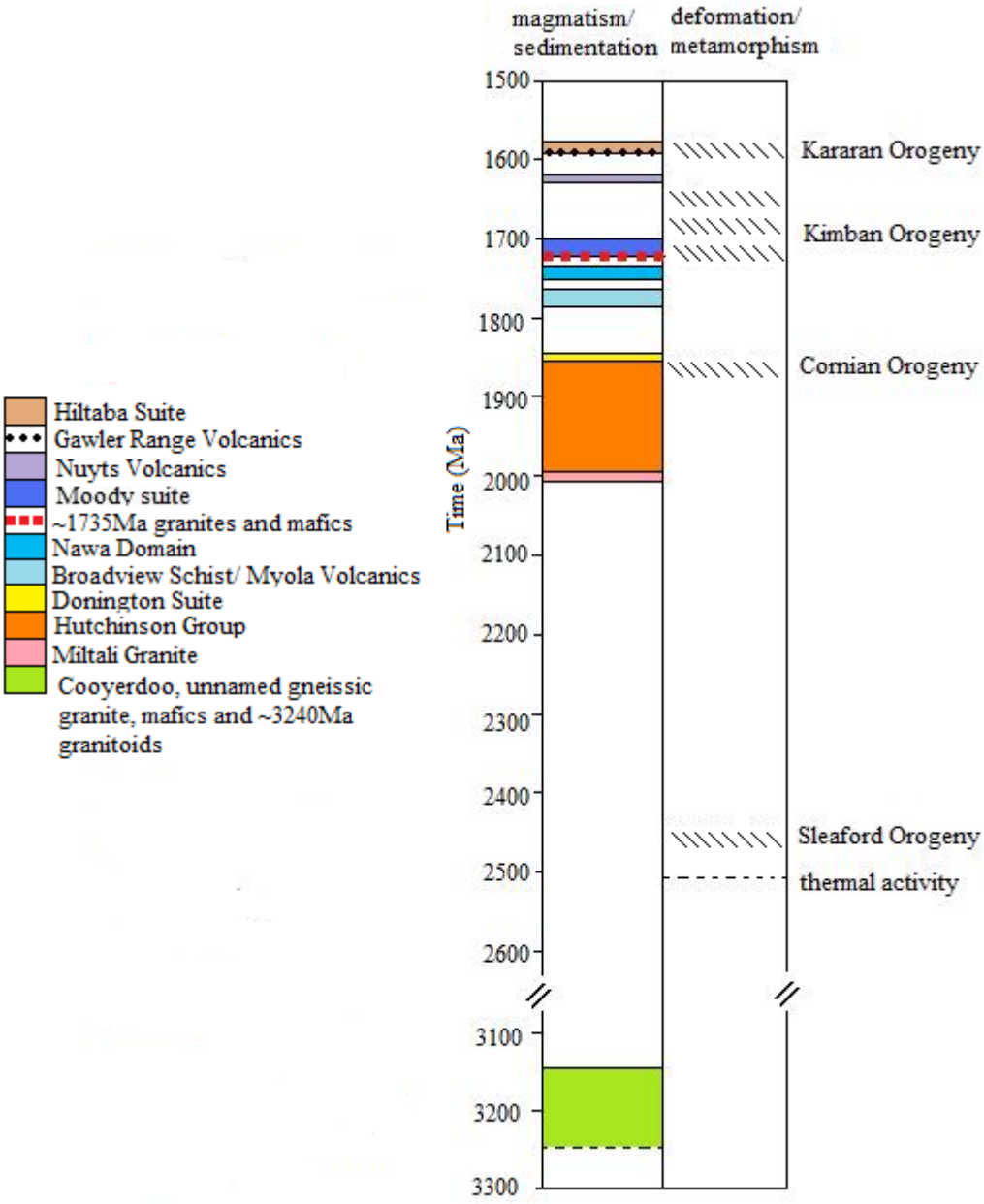
magmatism/
sedimentation
deformation/
metamorphism
Time (Ma)
1500
1600
1700
1800
1900
2000
2100
2200
2300
2400
2500
2600
3100
3200
3300
Kararan Orogeny
Kimban Orogeny
Cornian Orogeny
Sleaford Orogeny
thermal activity
Hiltaba Suite
Gawler Range Volcanics
Nuyts Volcanics
Moody suite
~1735Ma granites and mafics
Nawa Domain
Broadview Schist/ Myola Volcanics
Donington Suite
Hutchinson Group
Miltali Granite
Cooyerdoo, unnamed gneissic granite, mafics and ~3240Ma granitoids

Figure 2

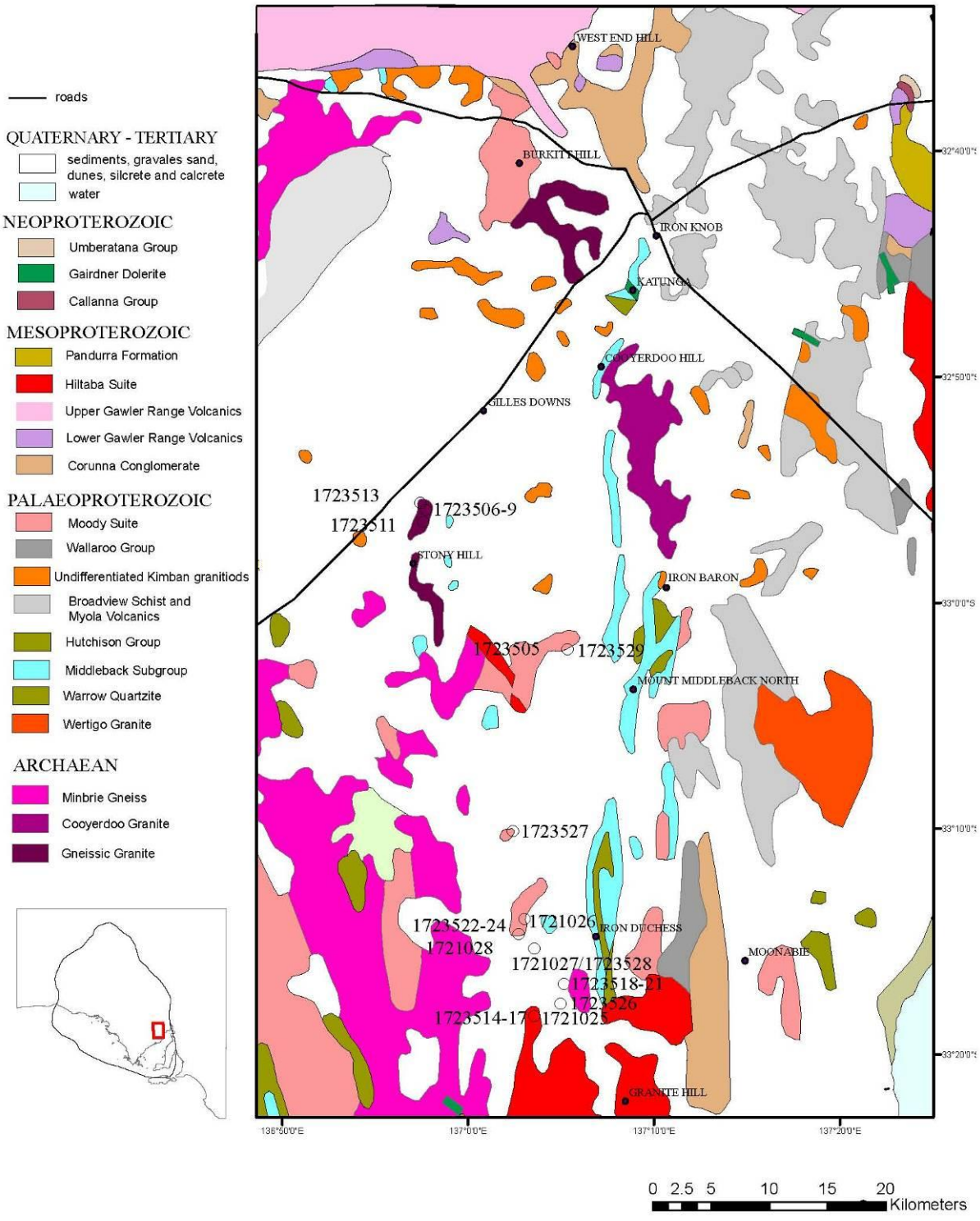
roads
QUATERNARY - TERTIARY
sediments, gravales sand, dunes, silcrete and calcrete
water
NEOPROTEROZOIC
Umberatana Group
Gairdner Dolerite
Callanna Group
MESOPROTEROZOIC
Pandurra Formation
Hiltaba Suite
Upper Gawler Range Volcanics
Lower Gawler Range Volcanics
Corunna Conglomerate
PALAEOPROTEROZOIC
Moody Suite
Wallaroo Group
Undifferentiated Kimban granitiods
Broadview Schist and Myola Volcanics
Hutchison Group
Middleback Subgroup
Warrow Quartzite
Wertigo Granite
ARCHAEAN
Minbrie Gneiss
Cooyerdoo Granite
Gneissic Granite
WEST END HILL
BURKITT HILL
IRON KNOB
KATUNGA
COOYERDOO HILL
GILLES DOWNS
1723513
1723506-9
1723511
STONY HILL
IRON BARON
1723505
1723529
MOUNT MIDDLEBACK NORTH
1723527
1723522-24
1721026
IRON DUCHESS
1721028
1721027/1723528
MOONABIE
1723518-21
1723526
1723514-17
1721025
GRANITE HILL
136°50'0"E
137°0'0"E
137°10'0"E
137°20'0"E
32°40'0"S
32°50'0"S
33°0'0"S
33°10'0"S
33°20'0"S
0 2.5 5 10 15 20
Kilometers

Figure 3

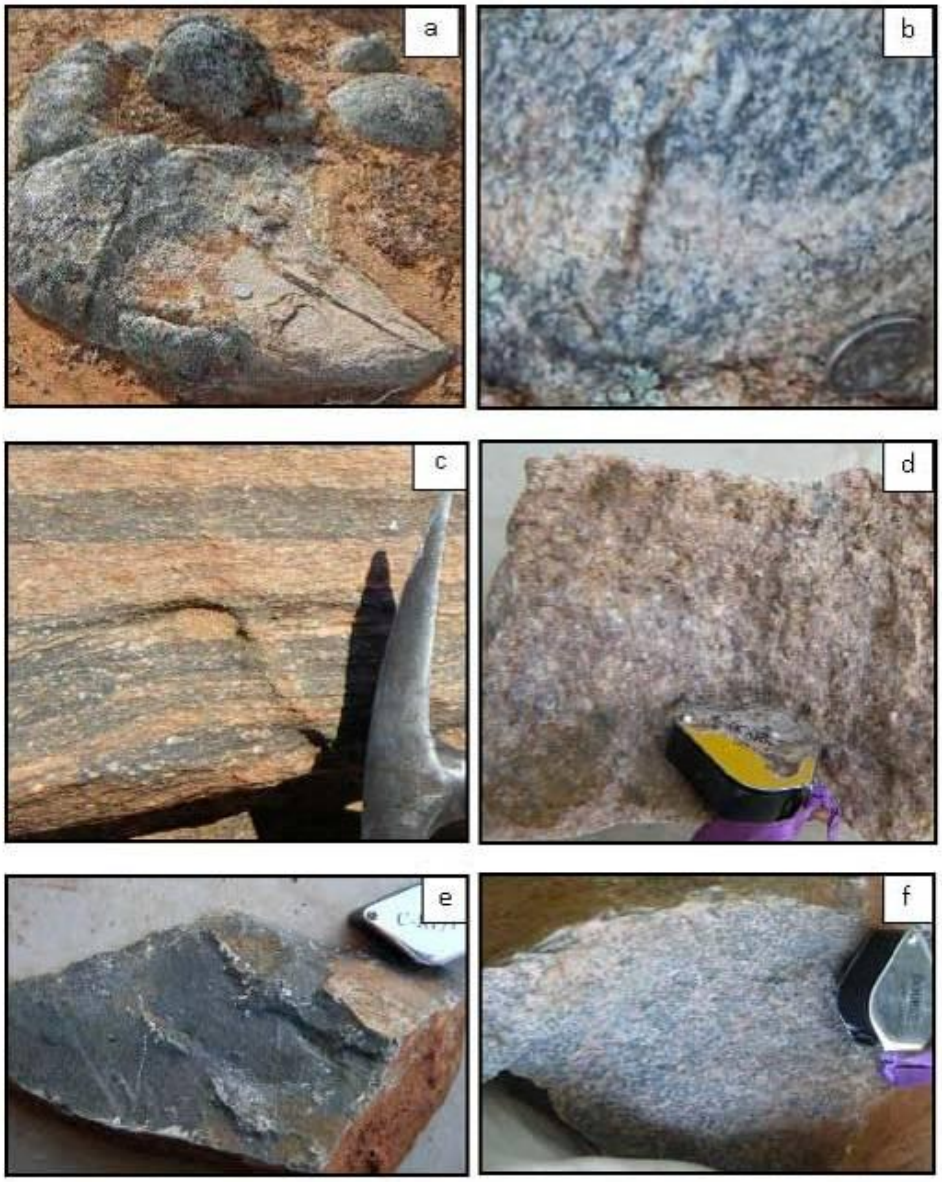

Figure 4

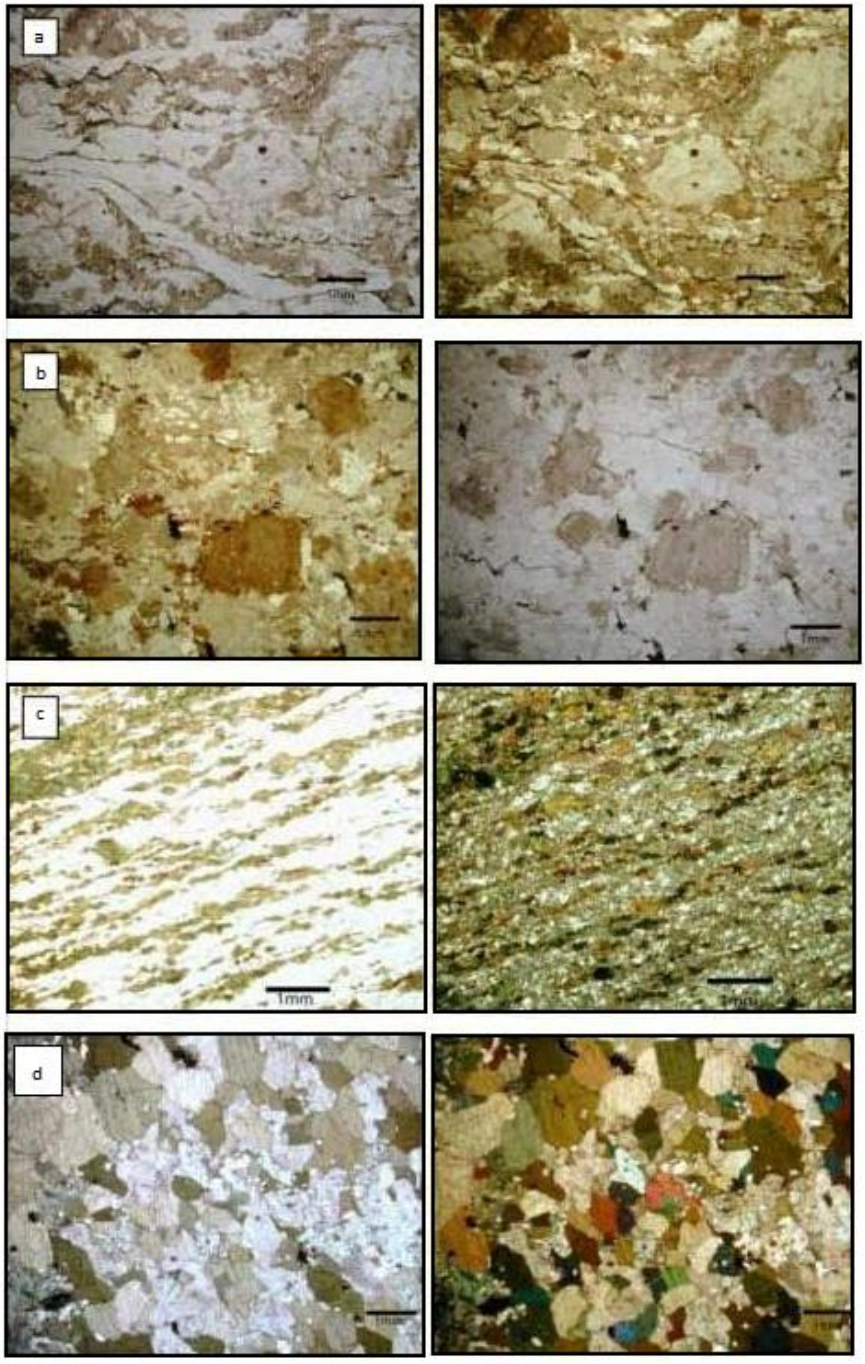

Figure 5

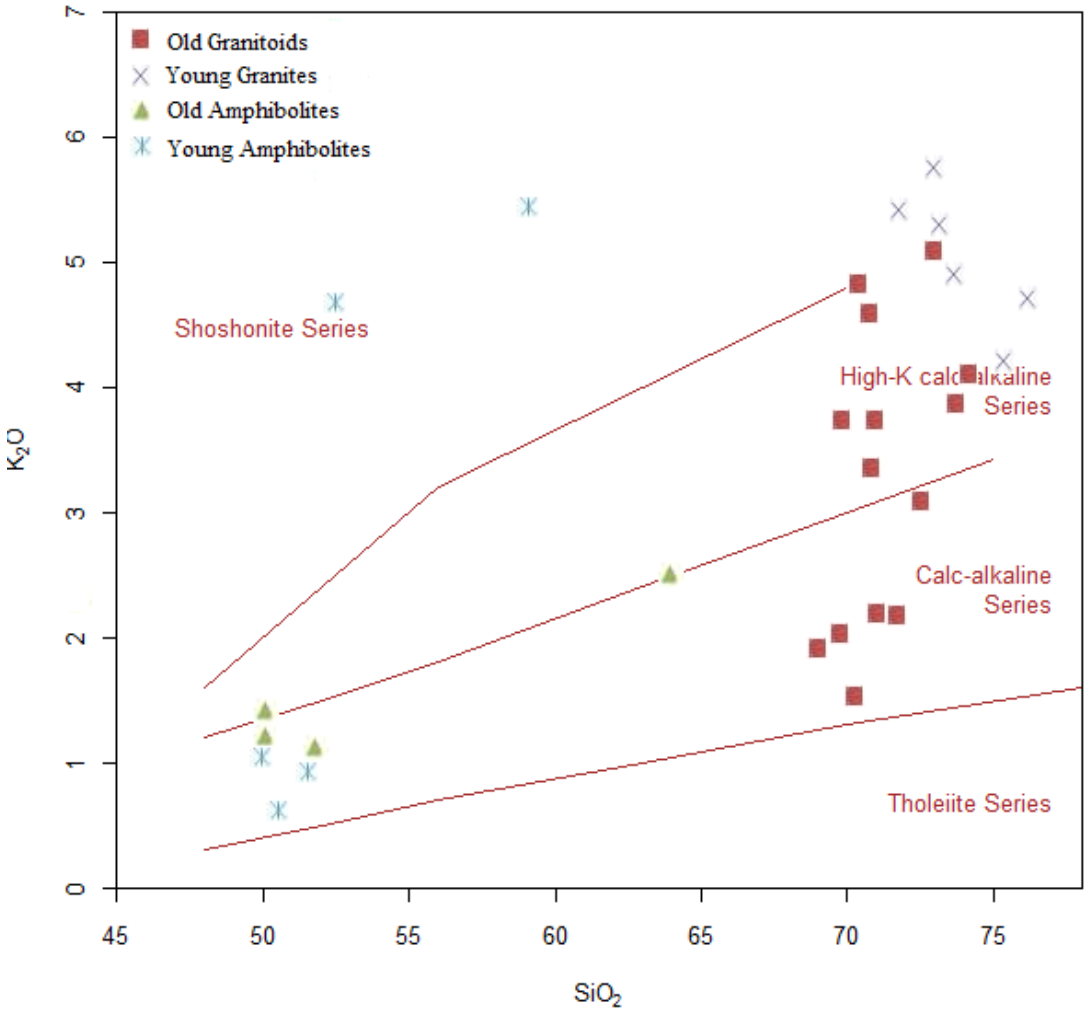
Old Granitoids
Young Granites
Old Amphibolites
Young Amphibolites
Shoshonite Series
High-K calc-alkaline Series
Calc-alkaline Series
Tholeiite Series
K_2O
SiO_2
0
1
2
3
4
5
6
7
45
50
55
60
65
70
75

Figure 6

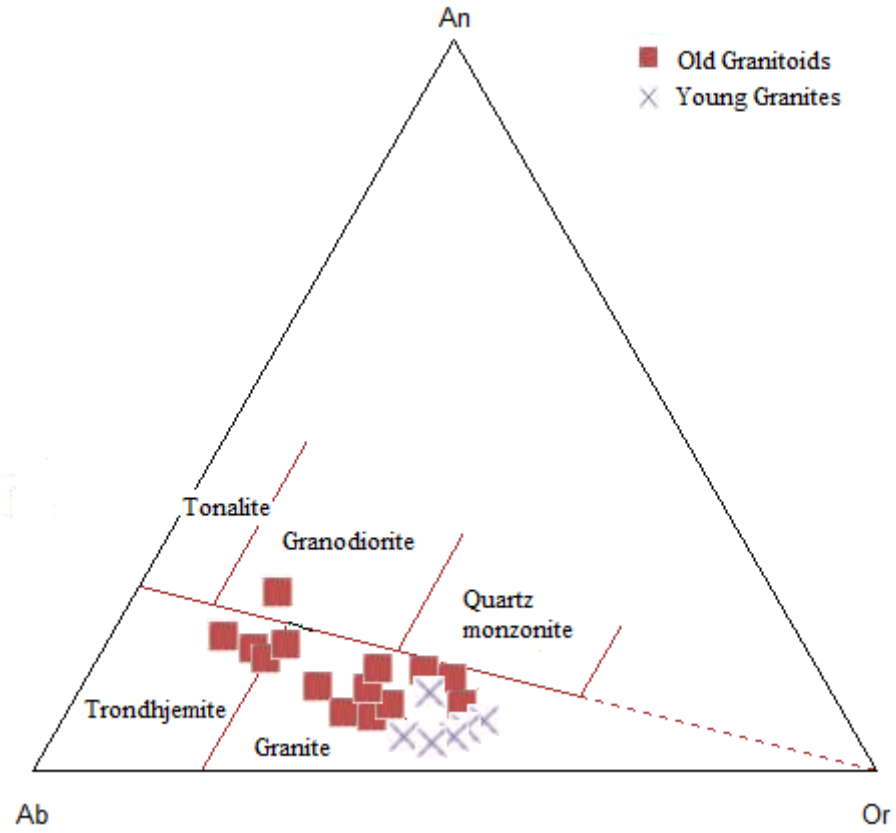
An
Old Granitoids
Young Granites
Tonalite
Granodiorite
Quartz
monzonite
Trondhjemite
Granite
Ab
Or

Figure 7

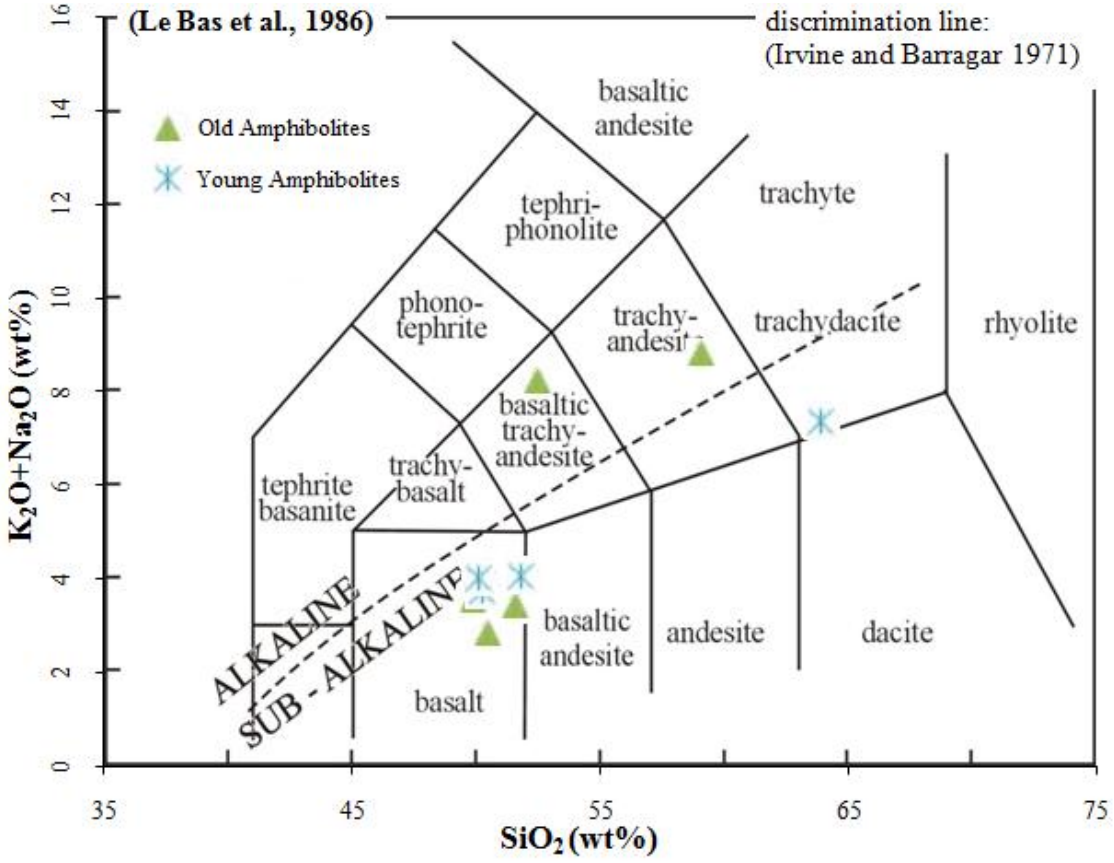
(Le Bas et al., 1986)
discrimination line:
(Irvine and Barragar 1971)
Old Amphibolites
Young Amphibolites
basaltic andesite
trachyte
tephri-phonolite
phono-tephrite
trachy-andesite
trachydacite
rhyolite
basaltic trachy-andesite
tephrite basanite
trachy-basalt
ALKALINE
SUB - ALKALINE
basaltic andesite
andesite
dacite
basalt
K_2O+Na_2O (wt%)
SiO_2 (wt%)
0
2
4
6
8
10
12
14
16
35
45
55
65
75

Figure 8

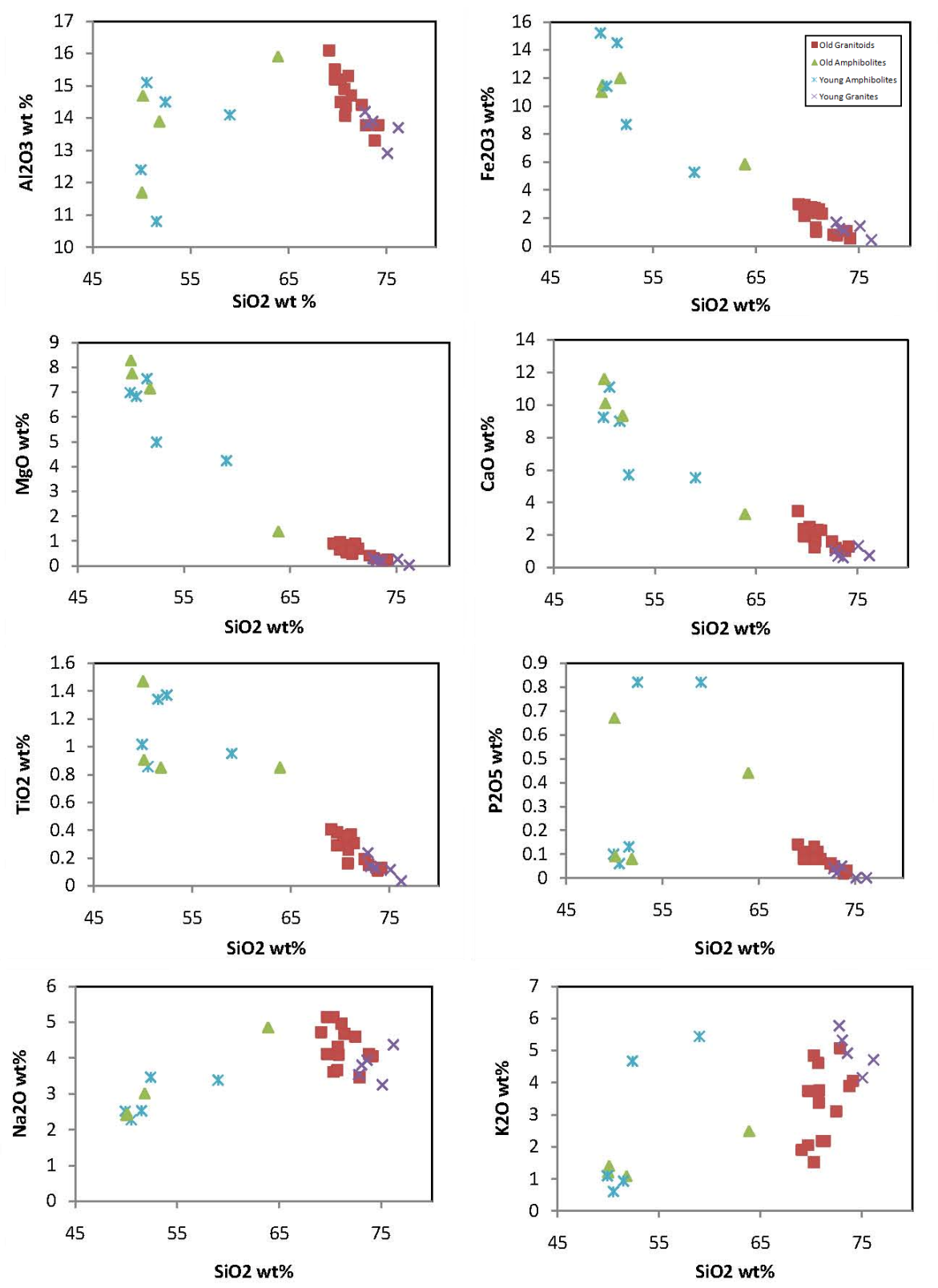
Al2O3 wt %
SiO2 wt %
Fe2O3 wt%
SiO2 wt%
Old Granitoids
Old Amphibolites
Young Amphibolites
Young Granites
MgO wt%
SiO2 wt%
CaO wt%
SiO2 wt%
TiO2 wt%
SiO2 wt%
P2O5 wt%
SiO2 wt%
Na2O wt%
SiO2 wt%
K2O wt%
SiO2 wt%

Figure 9

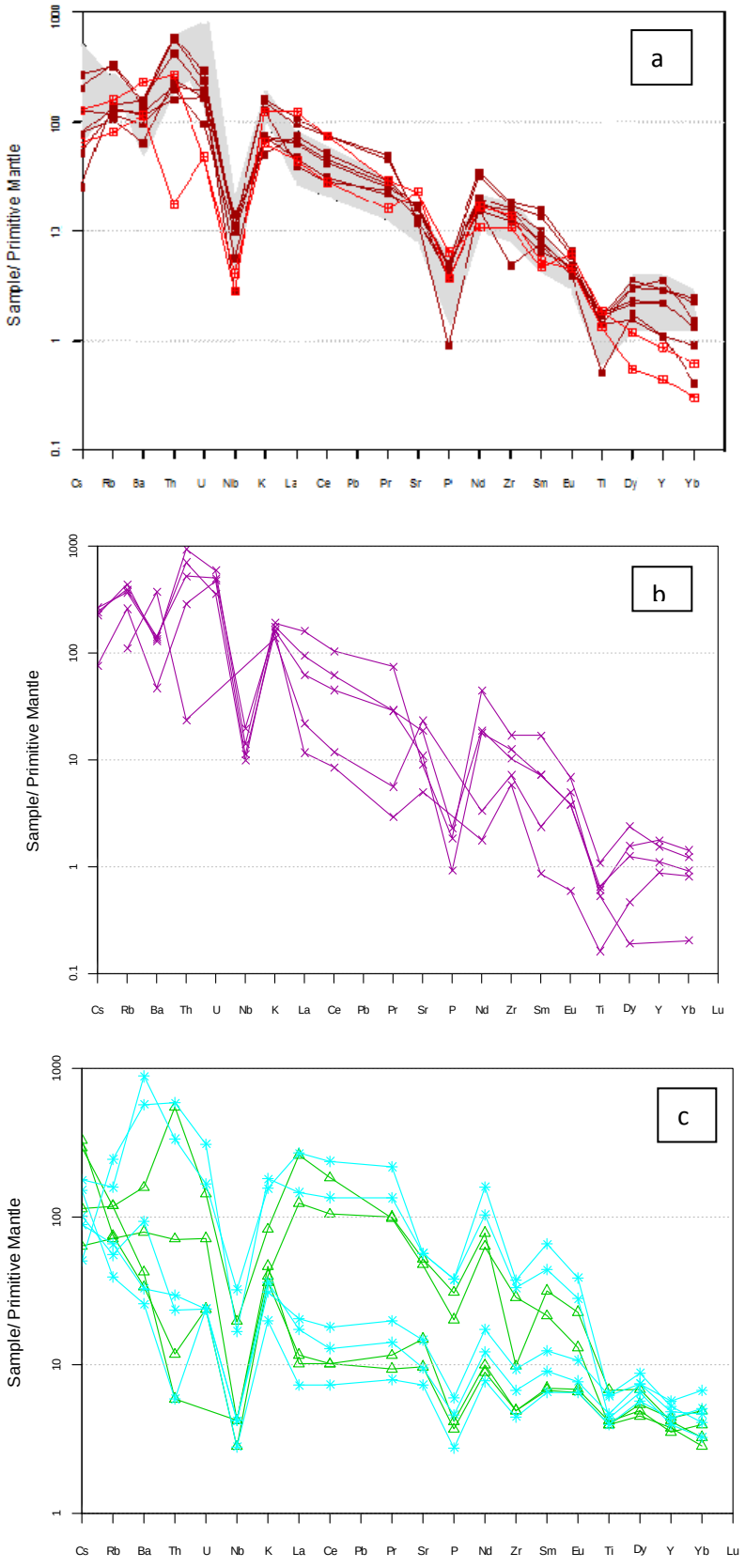
a
b
c
Sample/ Primitive Mantle
1000
100
10
1
0.1
Cs Rb Ba Th U Nb K La Ce Pb Pr Sr P Nd Zr Sm Eu Ti Dy Y Yb Lu

Figure 10

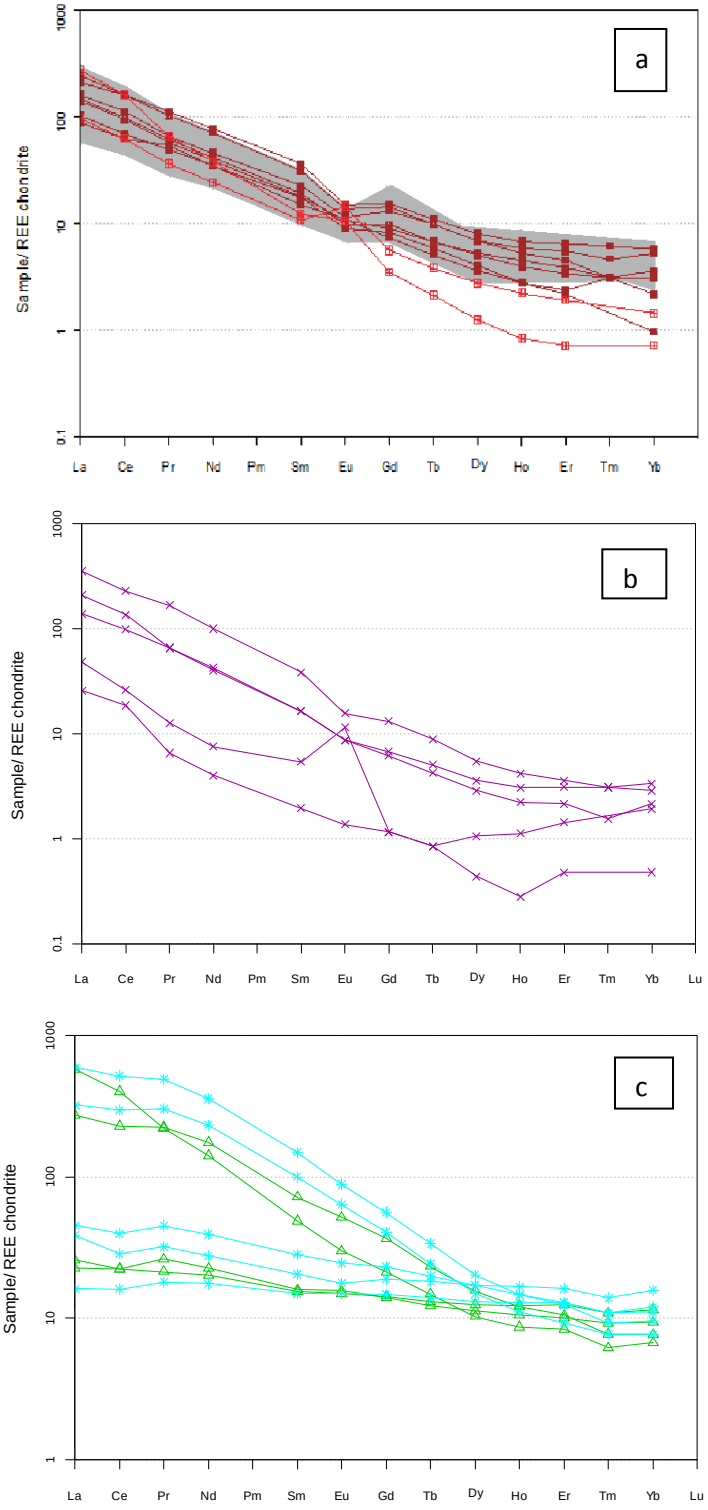
a
Sample/ REE chondrite
1000
100
10
1
0.1
La Ce Pr Nd Pm Sm Eu Gd Tb Dy Ho Er Tm Yb
b
Sample/ REE chondrite
1000
100
10
1
0.1
La Ce Pr Nd Pm Sm Eu Gd Tb Dy Ho Er Tm Yb Lu
c
Sample/ REE chondrite
1000
100
10
1
La Ce Pr Nd Pm Sm Eu Gd Tb Dy Ho Er Tm Yb Lu

Figure 11

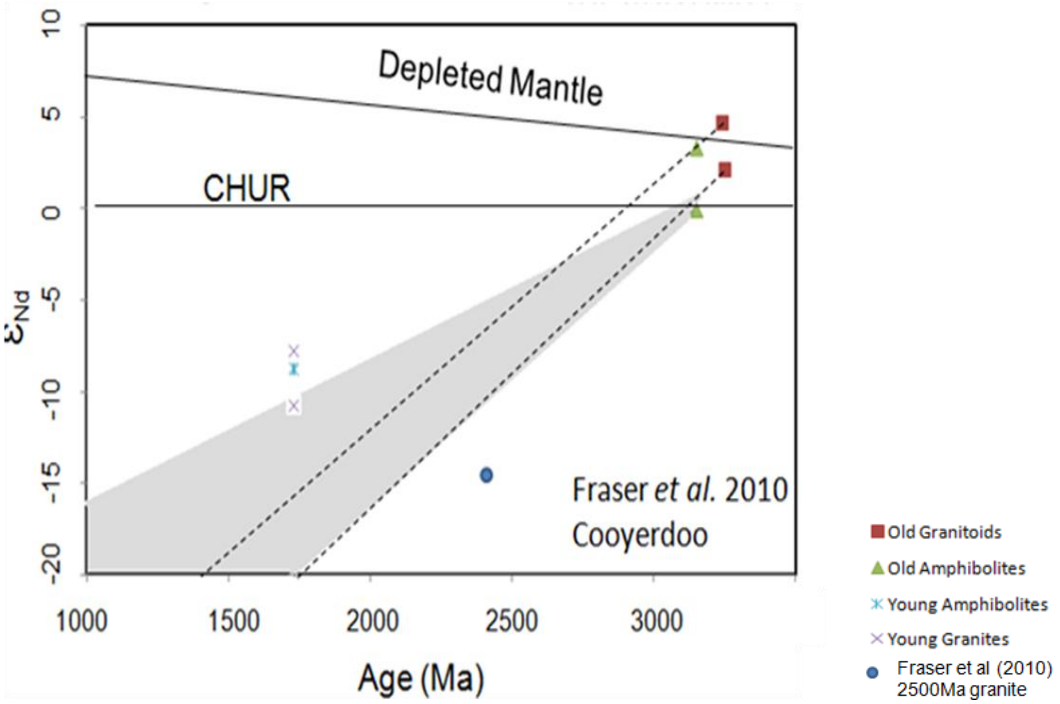
Depleted Mantle
CHUR
Fraser et al. 2010
Cooyerdoo
εNd
10
5
0
-5
-10
-15
-20
1000
1500
2000
2500
3000
Age (Ma)
Old Granitoids
Old Amphibolites
Young Amphibolites
Young Granites
Fraser et al (2010) 2500Ma granite

Figure 12

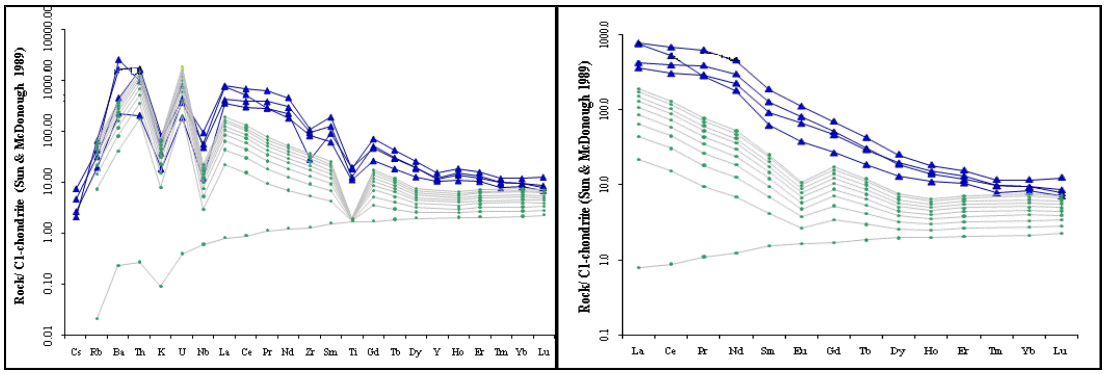
Rock/ C1-chondrite (Sun & McDonough 1989)
0.01
0.10
1.00
10.00
100.00
1000.00
10000.00
Cs Rb Ba Th K U Nb La Ce Pr Nd Zr Sm Ti Gd Tb Dy Y Ho Er Tm Yb Lu
Rock/ C1-chondrite (Sun & McDonough 1989)
0.1
1.0
10.0
100.0
1000.0
La Ce Pr Nd Sm Eu Gd Tb Dy Ho Er Tm Yb Lu

Figure 13:

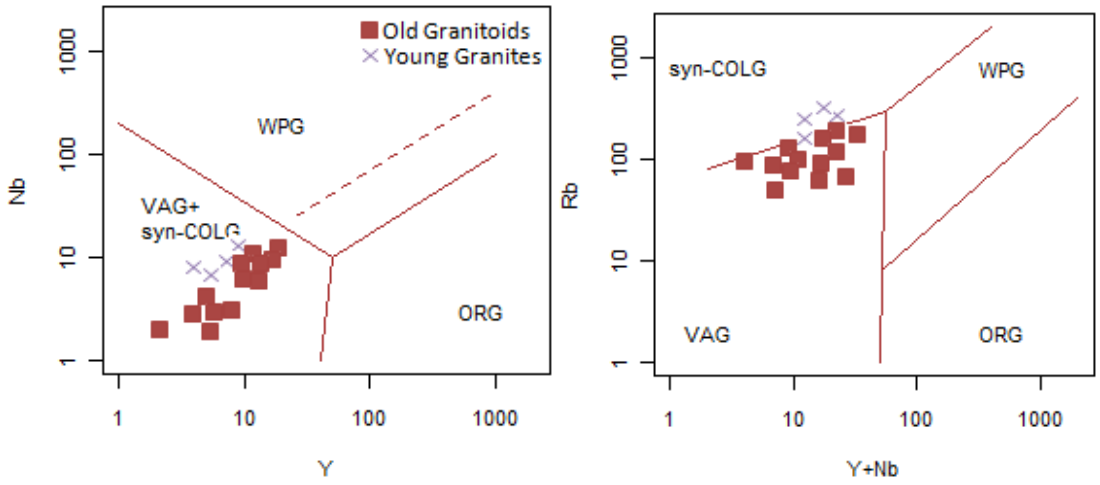
Old Granitoids
Young Granites
WPG
VAG+
syn-COLG
ORG
Nb
Y
1
10
100
1000
syn-COLG
WPG
VAG
ORG
Rb
Y+Nb

Figure 14

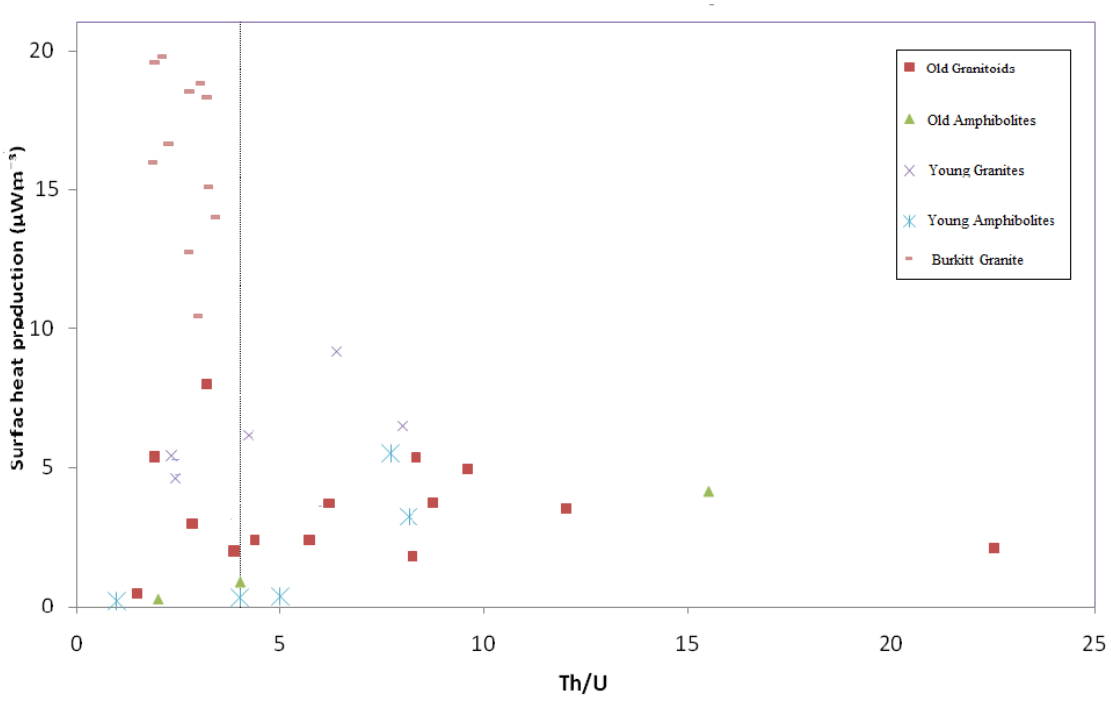
Surfac heat production (µWm⁻³)
Th/U
0
5
10
15
20
25
Old Granitoids
Old Amphibolites
Young Granites
Young Amphibolites
Burkitt Granite

Figure 15